INFLUENCE OF AN INTEGRAL SPLITTER PLATE AND AN ANNULAR FIN ON HEAT AND MOMENTUM TRANSPORT FOR THE CASE OF FLOW PAST A TUBE

By

Debadi Chakraborty

DEPARTMENT OF MECHANICAL ENGINEERING

Indian Institute of Technology Kanpur

FEBRUARY, 2003

INFLUENCE OF AN INTEGRAL SPLITTER PLATE AND AN ANNULAR FIN ON HEAT AND MOMENTUM TRANSPORT FOR THE CASE OF FLOW PAST A TUBE

A THESIS SUBMITTED

IN PARTIAL FULFILMENT OF THE REQUIREMENTS

FOR THE DEGREE OF

MASTER OF TECHNOLOGY

BY

DEBADI CHAKRABORTY

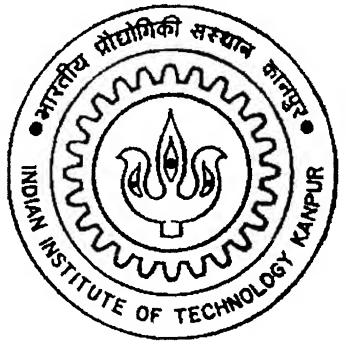

DEPARTMENT OF MECHANICAL ENGINEERING

INDIAN INSTITUTE OF TECHNOLOGY KANPUR

February 2003

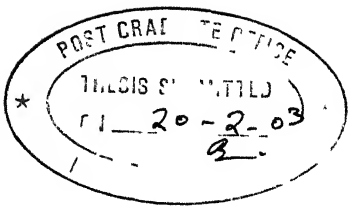

Certificate

This is to certify that the thesis entitled "**Influence of an Integral Splitter Plate and an Annular Fin on Heat and Momentum Transport for the Case of Flow Past a Tube** " by Mr Debadi Chakraborty has been carried out under our supervision The contents of this thesis have not been submitted to any other Institute or University for the award of any degree or diploma

Dr Gautam Biswas
Department of Mechanical Engineering
Indian Institute of Technology
Kanpur-208016

Dr P K Panigrahi
Department of Mechanical Engineering
Indian Institute of Technology
Kanpur -208016

February 20,2003

Abstract

Influence of an Integral Splitter Plate and an Annular Fin on Heat and Momentum Transport for the Case of Flow Past a Tube

The longitudinal finning of a circular tube is assumed to be in a configuration where the fin is attached at the back of a circular tube The longitudinal fin, attached at the back of the tube, is called integral splitter plate The flow and heat transfer results are presented for three different lengths (L=2H, 3H and 4H) of the splitter plate and three different Reynolds numbers (500, 1000 and 1500) A splitter plate or longitudinal fin connected integrally to a circular tube (behind the tube) plays an important role in reducing the size of the wake zone The flow physics of such a system becomes quite interesting The role of the splitter plate in heat transfer enhancement is an important aspect to be investigated The wake of a circular tube without a splitter plate removes heat from the tube surface more effectively as compared to the present case of tube with splitter plate However the combined effect of conduction and convection in the latter case is certainly greater than that of the former one

We focus our attention on a section where only one annular fin has been considered The geometry of interest is basically a representative section whereby the length of the tube is equal to the pitch of the annular fins Appropriate grid is generated and computations are carried out for $Re_H = 1000$ The effect of annular fin on heat transfer and flow characteristics is to be compared with the heat transfer and flow characteristics for the case of a circular tube The results are presented for annular fin of outer diameter 1 5 times the diameter of the tube

Acknowledgements

I express my sincere gratitude, regards and thanks to my thesis supervisors Prof Dr G Biswas and Dr P K Panigrahi for their excellent guidance, invaluable suggestions and generous help at all the stages of my research work Their interest and confidence in me was the reason for all the success I have made

I am extremely grateful to my friends Tathagato Bhattacharya, Mukesh Gupta, A K Sharma and Abhishek Jain for all the encouragement and support I have received from them at all times I am glad to record my thanks to my colleagues at CFD lab whose kindness and cooperation, I remember with gratitude I am thankful to Abhinandan Agrawal, Shaligram Tiwari, Suman Basu, Aseem Jain, Dalton Mourya, Somnath Roy, Santanu De, Deepak Agarwal, Neetu Srivastava and Jawahar Pandey

Once again, I would like to thank all my classmates for their smile and friendship making the life at I I T Kanpur enjoyable and memorable

I shall be always greateful to those invisible persons whose support can not be expressed in words

Debadi Chakraborty

February, 2003
IIT Kanpur

Contents

List of Figures

Nomenclature

CV	control volume
C_p	specific heat at constant pressure
k	thermal conductivity
Nu	local Nusselt number i e $(\partial\theta/\partial Z)_{Z=w}$
Nu_m	Mean Nusselt number
p	static pressure
p_∞	inlet pressure
U_∞	inlet velocity
T_∞	atmospheric temperature
T_W	wall temperature
Re_H	Reynolds number based on channel height i e $\rho U_{av} H/\mu$
Re_D	Reynolds number based on tube diameteri e $\rho U_{av} D/\mu$
S	surface area of a cell face
t	time
u	axial component of velocity
v	spanwise component of velocity
w	normal component of velocity
x	axial dimension of coordinates
y	spanwise dimension of coordinates
z	normal dimension of coordinates

L_1	axial dimension of computational domain
L_2	spanwise dimension of computational domain
l_C	distance of center of tube from the inlet
H	height of the tube
L	fin length
D	tube diameter
D_1	outer diameter of the annular fin
X, Y, Z	non-dimensional coordinates corresponding to x,y and z respectively
T	temperature
$\mathbf{v}$	velocity vector
(x, y, z)	position in Cartesian coordinates

Greek

α	Thermal diffusivity
γ	upwinding factor
θ	non-dimensional temperature i e $(T - T_\infty)/(T_w - T_\infty)$
μ	viscosity of the fluid
ρ	density of the fluid

Subscripts

b	bulk condition
j	cell face
i	cell center
w	wall

Superscripts

$n, n+1$	time level

Chapter 1

Introduction

1.1 Problem Description

Fin-tubes are commonly used in many gas-liquid cross-flow heat exchangers In such an arrangement, the cold stream (gas) generally flows across outside the tubes and the hot fluid (often it is liquid) flows inside the tubes The fins provide the extra heat transfer surface area for the cold fluid Even with the extended surfaces, the dominant thermal resistance in air cooled condensers is on the air side, since condensation (phase-change heat transfer) takes place inside the tubes Therefore, in order to achieve significant heat transfer enhancement, strategies must be developed, that would result in increased heat transfer coefficients on the fin and the tube outer surfaces without a large increase in pressure drop.

Figure 1 1 shows a schematic diagram of the core region of a fin-tube heat exchanger Numerical investigations in this field have been carried out by Biswas et al (1994), where they have tried to achieve the enhancement of heat transfer from the fin surfaces by inducing longitudinal streamwise vortices in the flow field These vortices were generated with the help of delta-winglet type vortex generators on the flat surface(Figure 1 2) The longitudinal vortices are developed along the side edge of the delta-winglets due to pressure difference between the front surface facing the flow and the back surface Such vortices are also called

streamwise vortices because they have axes parallel to the flow direction Once they get developed, they interact with an otherwise a two-dimensional boundary layer and produce a three-dimensional swirling flow that mixes near wall fluid with the free stream This is a type of kinematic mixing and strongly enhances the entrainment of fluid from periphery to the core region of the flow field It results in disruption of thermal boundary layer which causes enhancement of heat transfer The additional pressure losses happen to be modest because the form drag for such winglet-type slender bodies is low

In the present work numerical simulations have been carried out for flow and heat transfer in fin-tube cross-flow heat exchangers We have considered two different flow configurations In one case longitudinal fin is attached at the back of a tube and in another annular fins are attached on the tube The grid-mesh used is of body-fitting type employing finite volume algorithm of Eswaran and Prakash (1998)

1.2 The Scope of Present Work

In order to achieve the objective outlined obove, a numerical investigation has been carried out The complete Navier-Stokes equations together with the energy equation are solved in a rectangular channel with a built-in circular tube having a longitudinal fin, i e , Splitter Plate and built-in circular tube having a circumferential fin, i e , Annular Fin A detailed analysis of the flow structure together with heat transfer characteristics in such modules have been performed.

1.3 Outline of the Thesis

In Chapter-1, the genesis of the problem has been discussed The Chapter-2 of the thesis provides a review of the literature relevant to understanding of the basic mechanism involved in augmentation of heat transfer, flow and the algorithms related to solving the Navier-Stokes equations The mathematical formulation of the problem for simulation is presented in Chapter-3 In this Chapter, the flow geometry, the governing equations, boundary conditions and grid generation techniques are discussed Chapter-4 discusses the solution algorithm and all the basic description of the finite volume formulation in detail Chapter-5 is divided into two sections In the first section a detailed study of flow physics and associated heat transfer are discussed for the case of a circular tube with an integral splitter plate and in the second section the same is discussed for the case of a circular tube with an annular fin Chapter-6 includes the concluding remarks and the scope for future research

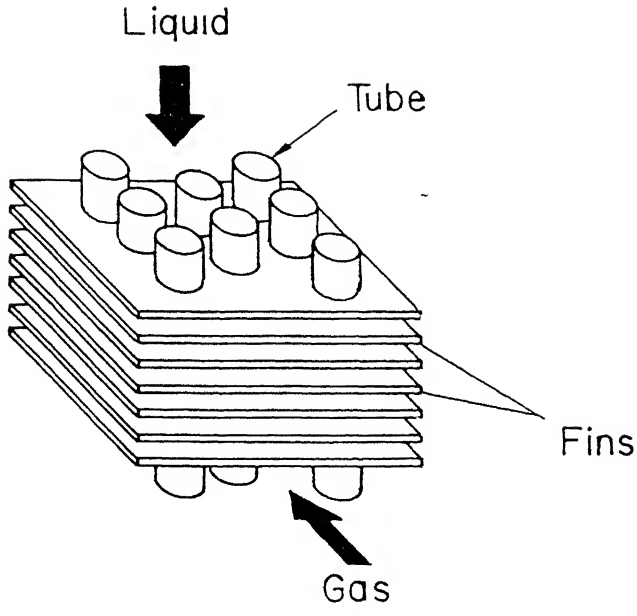

Figure 1 1 Schematic diagram of core region of a fin-tube heat exchanger

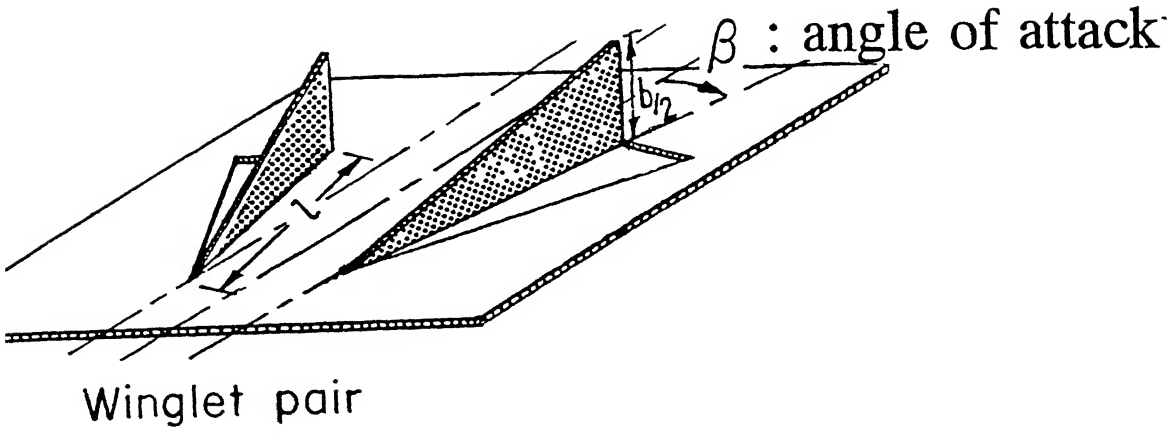

Figure 1 2 Delta-Winglet type vortex generators on flat surface

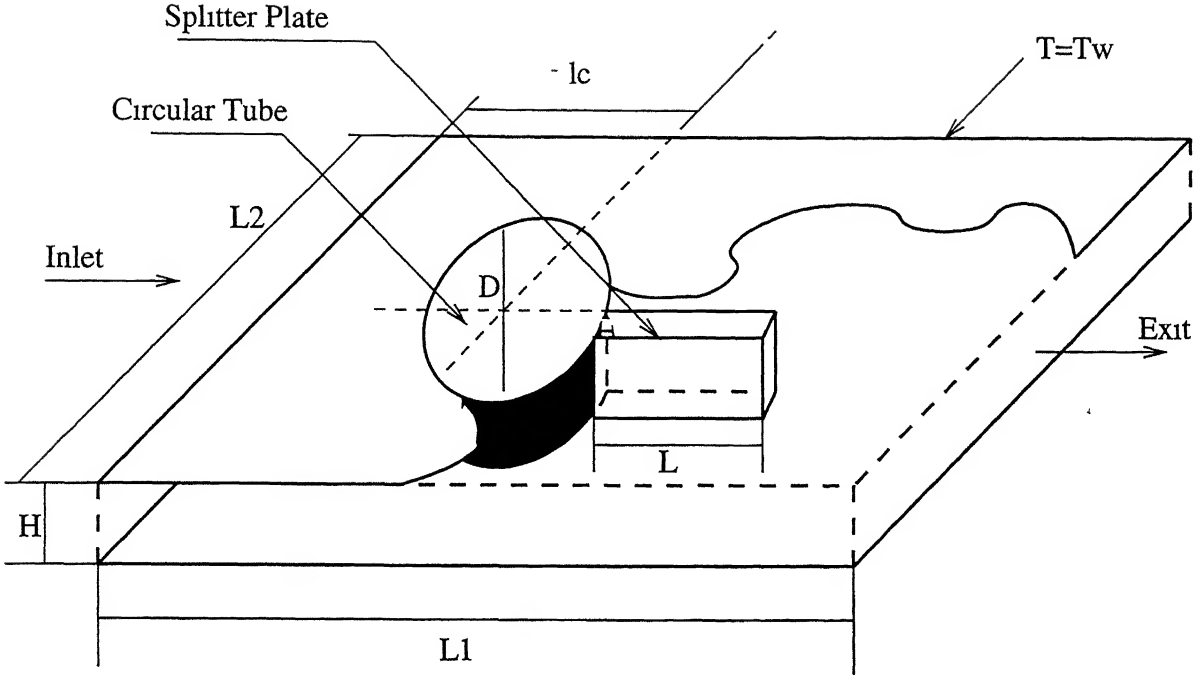

Figure 1 3 Three-dimentional Computational Domain for Splitter Plate

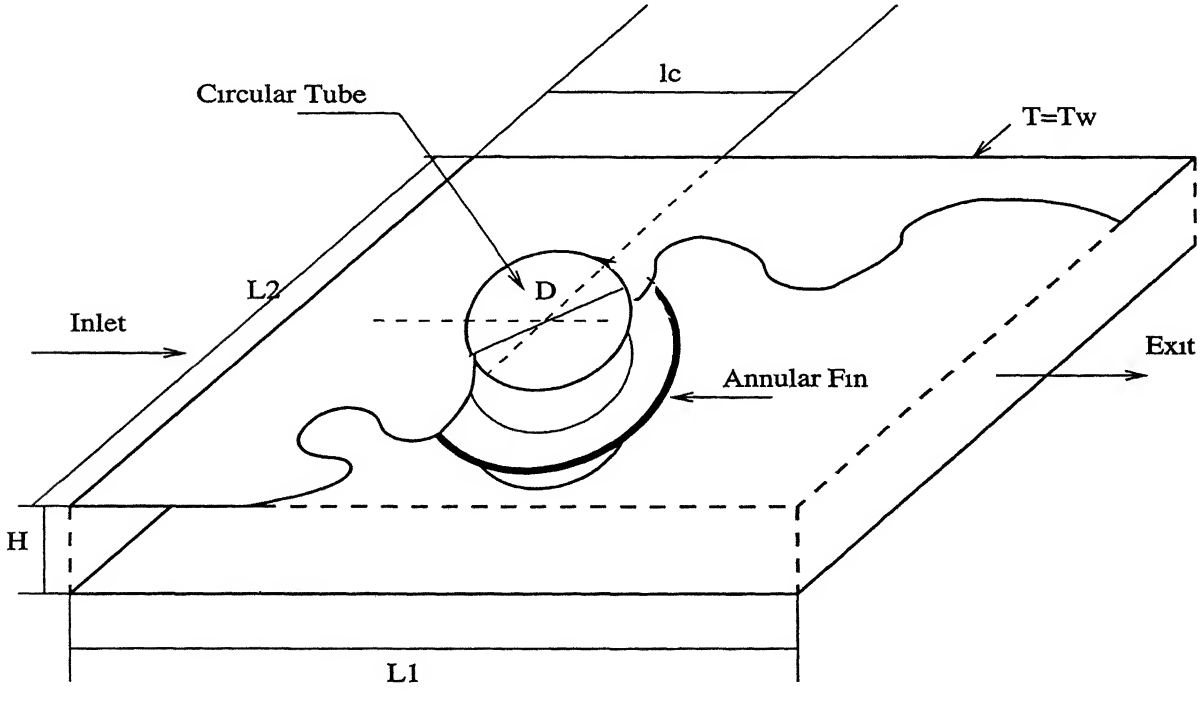

Figure 1 4. Three-dimentional Computational Domain for Annular Fin

Chapter 2

Literature Survey

2.1 Introduction

Considerable amount of experimental, analytical and computational research has been carried out on enhancement of heat transfer The enhancement of heat transfer through manipulation of surface geometry has been analyzed by many researchers and practitioners In order to analyze the flow structure and heat transfer in such applications, a detailed computational study is needed The flow regime may possess either laminar or turbulent characteristics Numerical solutions for laminar flows and heat transfer have been well developed by various researchers but the corresponding investigations for turbulent flows involve more rigorous considerations This chapter outlines a summary of articles available in the areas closely related to the present investigations The review of literature is divided in to three different sections In the first section, an overview of work done by various researchers in the area of enhancement of heat transfer and flow structures are presented There are three subsections in the first section The first subsection focuses on studies pertaining to the Vortex Generators The second one describes the work related to integral Splitter Plates and the third one is on Annular Fin The second section focuses on the numerical methods with regard to the task of computing flow fields in complex geometries Finally the benefits of current problem is established from the available knowledge of existing literature

2.2 Enhancement of Heat Transfer and Effect on Flow Characteristics

The primary interest of our present work is to enhance the heat transfer in the gas side of fin-tube heat exchangers keeping the pressure-drop penalty at a modest level With this intent, we would like to study different investigations related to augmentation of heat transfer suitable for the applications enumerated earlier Augmentation of heat transfer is of special interest in channel flows where the rate of heat transfer between the fluid and channel walls deteriorates as the boundary layer grows on the channel walls and the flow tends to become fully developed Protrusions can be mounted on these channel walls in order to disrupt the growth of boundary layer and thereby enhance the heat transfer between the flowing fluid and channel walls. Two relevant applications using such flow configurations are the heat transfer between the gas and the fin in the case of gas-liquid fin-tube crossflow heat exchangers and the heat transfer between the flowing fluid and plates in the case of fin-plate heat exchangers

2.2.1 Vortex Generators

The use of a multi-layered surface geometry for plates can disturb evolution towards a fully developed flow A detailed performance data for louvered fin surfaces is provided by Achaichia and Cowell (1988) In the louvered fins, enhancement in heat transfer is obtained at the cost of a high pressure drop In order to circumvent this difficulty, protrutions in the form of slender delta-winglets can be mounted on the fin surfaces (Figure 1 2) As shown, the base of the wing remains attached to the fin and the apex faces the incoming stream with an angle of attack The longitudinal vortices are generated along the side edge of the wing-shaped vortex generator due to the pressure difference between the front surface facing the flow and the back surface These longitudinal vortices, generated by the vortex generators, can be made to disturb the growth of boundary layer in a channel by exchanging the fluid from the near-wall-region with the channel-core-

region and thus they can serve to enhance the heat transfer rate while producing less of a pressure drop Use of longitudinal vortices for boundary control is well known(Pearcey, 1961) and the vortex generators are used in commercial airplanes for this purpose

Detailed investigation of the enhancement potential of vortex generators have been carried out in the last two decades (Fiebig et al (1986), Turk and Junkhan (1996), Eibeck and Eaton (1986), Fiebig et al (1989), Amon (1989), Dong (1989), Zhang (1989), Tigglebeck (1992), Yanagihara and Torii (1990), Fiebig et al (1990),Fiebig et al (1991), Sanchez (1989), Valencia (1992), Biswas et al (1994) and Valencia (1996)) The idea of using vortex generators in heat exchanger is being attempted by the industry Transverse vortex generators, such as ribs and corrugations in channel generate vortices whose axes are mainly transverse to the primary flow direction, whereas, longitudinal vortex generators, such as delta wings and rectangular wings generate vortices having axes along the primary flow direction The experimental and numerical investigations conducted so far show that the longitudinal vortex generators are better options as compared to the transverse vortex generators for improvement of heat transfer surfaces in the heat exchangers when both heat transfer enhancement and flow loss are taken into account

2.2.2 Splitter Plate

Experiments reported by a number of authors have shown that the characteristics of the separated wake downstream from a bluff cylinder can be greatly affected when a splitter plate is placed along the centerline of the wake. When a splitter plate is placed downstream of a circular cylinder in a crossflow at Reynolds numbers (at which a regular vortex street is shed from the plane cylinder), the vortex

shedding may be altered or even suppressed and the drag force experienced by the cylinder may be affected

Roshko (1954) did experiments with splitter plate in the wake of a circular cylinder in a two-dimentional cross flow at a Reynolds number of $1\ 45 \times 10^4$ He found that a splitter plate of length $5D$ (where D is the diameter of the cylinder)in contact with cylinder inhibited the periodic vortex formation and caused the reduction in pressure drag experienced by the cylinder A splitter plate of length $1\ 14D$ in contact with the cylinder did not inhibit the vortex formation, but it caused an increase in the base pressure and a reduction in the Strouhal number as compared with the cylinder alone Roshko observed a complicated and interesting sequence of changes in the base pressure on the cylinder surface and in Strouhal number when he moved the shorter splitter plate downstream, leaving a gap between it and the cylinder

Gerrard (1966) measured the frequency of vortex shedding from a circular cylinder in a cross-flow at Reynolds number of 2×10^4 with splitter plate of different lengths upto a maximum of $2D$ attached to the cylinder As the splitter plate length was increased, the Strouhal number was found to decrease to a minimum of $St = 0.18$ for a plate length of approximately D Further increase in length beyond $L/D = 1$ resulted in a progressive increase in shedding frequency

Apelt and Isaacs (1970) found that short splitter plates attached to a circular cylinder in a cross-flow at a Reynolds number of $1\ 58 * 10^4$ caused large reduction in drag With a splitter plate of length $0\ 125D$ the pressure drag was reduced to 83% of the value measured for the plain cylinder For a splitter plate length of D the pressure drag was reduced to 68% of the plain cylinder value, but only relatively small further changes in drag resulted when the splitter plate length was increased in steps up to $8D$

Apelt et al (1973) studied experimentally the effect of splitter plates on the flow past a circular cylinder in the range of $10^4 < Re < 5 \times 10^4$ They concluded that the splitter plates reduce the drag markedly by stabilizing the separation points and produce a wake narrower than that for the case of cylinder alone The splitter plates raise the base pressure by as much as 50% and affect the Strouhl number to a lesser degree While C_D and St have minimum values at about $L/D = 1$, the base pressure, C_p was maximum

Sparrow and Kang (1985) conducted experimental investigations on longitudinally-finned cross-flow tube banks and studied heat transfer and pressure drop characteristics They showed that a high degree of heat transfer enhancement was obtained by finning the tubes The finning related enhancements were compared with those attainable by increased diameter unfinned tubes Finning was found especially advantageous when the comparison was made at a fixed pressure drop They considered longitudinal fins at the front, at the rear or both at front and rear The rearward fins, which are basically wake splitters, produced a lower pressure drop than all other arrangements The experiments were carried out in the Reynolds number (based on tube diameter) range of 1200 to 8600

Mansingh and Oosthuizen(1990) carried out experimental study for the effect of splitter plates on the wake behind a two-dimensional bluff body (a rectangular cylinder) with fixed separation points at low Reynolds numbers between 350 and 1150 The results indicated that splitter plates alter the manner of vortex formation in the wake causing a decrease in shedding frequency, an increase in base pressure and a reduction in the overall drag by nearly 50%

Anderson and Szewczyk (1997) conducted experiments in an atmospheric wind tunnel to study the near wake of a circular cylinder at subcritical Reynolds num-

bers between 2700 to 46000 A base mounted splitter plate allowed for the modification of the formation region characteristics without disrupting the normal Karman shedding Their results provided an explanation for the non-linearity in the relationship between shedding frequency and the splitter plate length In addition to the nominal 2-D configurations, a sinuous trailing edge Splitter Plate, cylinder taper and shear flow were incorporated to study the three-dimensionality

2.2.3 Annular Fin

Transverse annular-finned tubes are widely used as a means of enhancing covective heat transfer in a crossflow The flow around an annular-finned circular tube in a crossflow exhibits extremely complex three-dimentional flow characteristics Hyung et al (1995) carried out experiments for local mass transfer from a circular tube, which is situated between two annular fins in a crossflow, at a over moderate Reynolds numbers ($33 \times 10^3 < Re_D < 80 \times 10^3$) They employed naphthalene sublimation technique to measure the local convective mass transfer around the circular tube The ratio of axial gap distance between two axial fins (L) to the radial protrusion length of the annular fin (H)was an important experimental parameter and its range was $0 < L/H < 0\ 40$ They found that for a small gap distance ($L/H = 0.05$), naphthalene sublimation is intense in the front portion of the circular tube, especially near the separation region. When the gap distance is moderate ($L/H = 0\ 15$), the overall character of sublimation shows a more organized pattern. The influence of horseshoe vortices is substantial For a large distance ($L/H = 0\ 40$), the impact of horseshoe vortices on the corner junction in the vicinity of the endwall is substantial

Sparrow and Chastain (1986) conducted wind-tunnel experiments to investigate the sensitivity of the heat transfer coefficient for an annular fin to small angles

of attack ($-2^o < \alpha < 2^o$, α=angle of attack) They found that the heat transfer coefficient in forward zone of the tube was highly sensitive to the angle of attack, increasing by about 50% on the face of the fin where leading-edge separation was activated as the angle was varied from -2^o to 2^o The increase in heat transfer coefficient at the side of the tube and behind the tube were about 10% Their experiments showed that, for any angle of attack in the investigated range, the two-face average for each zone was not very different from the heat transfer coefficient for zero angle of attack They concluded that the ovarall heat transfer performance of an annular fin is not significantly affected by small departures of the angle of attack from zero and since the difference between the heat transfer coefficients for the two faces of the fin were found to be significant, measurement of the coefficient at only one face may yield erroneous results for the overall heat transfer performance

2.3 Numerical Methods for Solving Navier-Stokes Equation

Different solution techniques have been developed during the past three decades The solution techniques for incompressible flows do not have any explicit equation for pressure and so due to spatial coupling of pressure and velocity it becomes quite difficult to obtain direct numerical solutions For incompressible flow problems, pressure does not have the usual thermodynamical meaning Here it is a relative variable, which adjusts itself instantaneously for the condition of zero mass divergence to be satisfied at all computational cells The primitive variable formulation of the incompressible Navier-Stokes equations has following distinctive feature It is well-known that in an incompressible fluid the speed of the sound is treated to be infinite As a consequence, the pressure field cannot be calculated by an explicit time advancement procedure and so it requires at least a partially implicit determination which takes into account the coupling between the pressure and velocity fields as well as the effects of the velocity boundary

conditions This aspect is the most distinctive feature of the primitive variable formulation of the incompressible Navier-Stokes equations This pressure field can be conveniently computed using the strem-function-vorticity approach for two-dimentional flows but it again creates problem for computation of three-dimentional flows due to absence of single scalar stream function

Primitive variable approach can be employed for three-dimentional problems which can be followed without encountering non-physical wiggles in pressure distribution As a remedy, it has been suggested to employ a different grid for each variable Harlow and Welch (1965) have used such a staggered grid for the dependent variables in their well known MAC (Marker and Cell) method The MAC method of Harlow and Welch is one of the earliest and widely used explicit methods for solving the full Navier-Stokes equations In this method, solution of velocities are obtained using a two step procedure In the first step called the predictor step, the provitional values of velocity components are computed explicitly using advection, diffusion and pressure gradient of the earlier time steps This explicitly advanced provisional velocity field may not necessarily ensure a divergence free velocity field Hence, in the second step called the corrector step, the pressure and velocity components are corrected so that the velocity field satisfy the continuity equation This is done through the solution of a Poisson equation of pressure A relative technique, known as pseudo-compressibility method, developed by Chorin (1967) involves a simultaneous iteration of the pressure and velocity components. Vicelli (1971) has shown that the method due to Chorin (1967) and the MAC method are equivalent The original version of the MAC method has been modified by Harlow and Amsden, popularly known as Simplified MAC (SMAC, 1970)

Since implicit methods have no such restrictions, they are more attractive Patankar and Spalding (1972) have introduced an efficient method known as SIMPLE

(Semi-Implicit Method for Pressure Linked Equation) This method is based on a finite-volume discretization of the governing equations on a staggered grid In order to improve the convergence involved in the pressure-velocity coupling, several variants of SIMPLE algorithm have been developed The SIMPLER algorithm of Patankar (1981) and the SIMPLEC algorithm of Van Doormaal and Raithby (1984) are improvements on SIMPLE Although the changes to incorporate SIMPLEC into SIMPLE algorithm are minor, the consequences can be great as it eliminates the approximation made in SIMPLE while deriving the pressure-velocity corrections

Application of finite volume methods using non-orthogonal coordinates and collocated grids is reported by Rhie and Chow (1983) and Peric (1985) Ferziger and Peric (1999) have shown that collocated arrangement converges faster than the staggered variable arrangement and has advantages when extensions such as multigrid techniques and non-orthogonal grids are considered Mukhopadhyay et al (1993) has developed a numerical method for predicting viscous flows for incompressible geometries Integral mass and momentum conservation equations are developed and these are discretized into algebric form through numerical quadrature The physical domain is divided into a number of non-othogonal control volumes which are iso-parametrically mapped on to standard rectangular cells Numerical integration for unsteady momentum equation is performed over such non-orthogonal cells The results exhibit good accuracy and justify the applicability of the algorithm Kobayashi and Pereira (1991) had modified the momentum interpolation method suggested by Peric (1985) and named it as Pressure-Weighted Interpolation Method-Corrected (PWIMC) In this method, the non-orthogonal terms in the momentum equations were solved explicitly, whereas in the pressure-corrections they were droped

It is clear that subtantial progress has been made for the development of al-

gorithms for complex geometries incompressible flow simulations but none of the prescriptions is universal Depending on the nature of flow and geometry etc , one can always go for the best suited discretization procedure It is very difficult to conclude about any algorithm with its universal sense of applicability The finite volume algorithm developed by Eswaran and Prakash (1998) for solving time dependent three-dimensional full Navier-Stokes equation has following advantages It uses collocated grid arrangement, hence all the advantages of collocated grid arrangement are gainfully utilized The essence of the algorithm is SMAC so it is suitable for modeling unsteady flows (Kim and Benson, 1992) The governing equations are discretized in the physical plane itself without coordinate transformation This algorithm has been used to solve the flow problem and extended to solve energy equation for the present work

Peric et al (1988) carried out a comparative study of finite volume numerical methods with staggered and collocated grids They concluded that the collocated method possesses no disadvantage relative to the staggered grid version The treatment of boundary conditions and the implementation of higher order differencing schemes are simpler In some cases, the collocated version provides faster convergence. It behaves similar to the staggered version under the variation of grid and under-relaxation parameters, and provides solutions of equal accuracy at the same or lower computing cost

2.4 How the Current Problem Benefits form Existing Literature

The experiments of Sparrow and Kang (1985) and Apelt et al (1973) reveal the effective utilization of the splitter plate for the purpose of enhancement of heat transfer while producing less pressure drop Sparrow and Kang (1985) considered longitudinal fins at the front, at the rear or both at front and rear The longi-

tudinal fin attached at the rear are basically wake splitters The splitter plate creates a streamlined extension of the circular tube It brings about enhancemnet of heat transfer as well A reduction in the size of wake zone is observed Narrowing of the wake zone reduces convective heat transfer from the tube surface but splitter plate itself generates an extra fin area for conduction Overall, there is an improvement in heat transfer past the circular tube with integral splitter plate as compared to the case of flow past a plain circular tube

The experiments of Sparrow and Chastian (1986) reveal that an annular fin attached to a tube is not significantly affected by small departure of the angle of attack from zero as the two-face averaged heat transfer coefficient does not differ from the heat transfer coefficient for zero angle of attack

The air-cooled condensers of geothermal plants consist of the same fin-tube arrangements as shown in Figure 1 1 Large fans are used to force the air through several rows of these fin-tubes The overall cost of these type of plants is very much effected by this type of very large condensers In this present numerical study, two three-dimensional numerical models have been formulated to provide a better understanding of the heat and flow characteristics The complete Navier-Stokes equations together with the energy equation are solved for an element of heat exchanger Figure 1 3 is the schemetic representation of the module used for the case of a circular tube with an integral splitter plate In this case, the flow structure and heat transfer characteristics for three different lengths ($2H, 3H$ and $4H$) of the splitter plate have been analysed Figure 1 4 shows the module used for the case of a circular tube with an attached annular fin The influence of an annular fin, attached to the tube at the height of the mid-plane of the channel, have been studied

Chapter 3

FORMULATION OF THE PROBLEM

3.1 Introduction

The need to enhance the heat transfer in fin-tube heat exchangers so as to reduce their size and thereby cost, has led us to compute the flow and heat transfer characteristics in a horizontal channel having a built-in circular tube with a longitudinal fin and annular fin. This numerical study can provide information about the heat transfer enhancement in fin-tube heat exchangers and effect of various flow parameters

3.2 Statement of the Problems

3.2.1 Splitter plate

The computational domain for the present problem is shown in Figure 1 3 Computations are performed for a circular tube of diameter $D = 4\ 0H$, H being the height of the domain parallel to axis of the tube The domain length along flow direction is $L_1 = 20H$ and the width in transverse direction is $L_2 = 11\ 25H$ The center of the tube is at a distance $l_C = 6\ 4H$ from the inlet For a particular flow Reynolds number, different fin lengths are considered ($l = 2H, 3H$ and $4H$) for flow and heat transfer study. Again, for a particular fin length,

computations are performed to investigate the effect of variation of Reynolds number(Re_H=500, 1000 and 1500) on the behavior of heat transfer Air has been considered as the working fluid, hence the Prandtl number is taken as 0 7 The tube and the longitudinal fin (splitter plate) are considered to be isothermal surfaces

3.2.2 Annular Fin

The computational domain is shown in figure 1 4 Computations are performed for a circular tube of diameter $D = 4\,0H$, H being the height of the domain parallel to axis of the tube The domain length along flow direction is $L_1 = 25H$ and the width in transverse direction is $L_2 = 12\,5H$ The center of the tube is at a distance $l_C = 8\,4H$ from the inlet The outer diameter of the annular fin is D_1=1 5D and Reynolds number is Re_H=1000 for flow and heat transfer study Air has been considered as the working fluid, hence the Prandtl number is taken as 0 7

3.3 Governing Equations

The three-dimensional continuity, Navier-Stokes and Energy equations for laminar flow of an incompressible fluid having uniform density are

$$\frac{\partial u_i}{\partial x_i} = 0 \tag{3 1}$$

$$\frac{\partial u_i}{\partial t} + u_j \frac{\partial u_i}{\partial x_j} = -\frac{1}{\rho}\frac{\partial p}{\partial x_i} + \nu \frac{\partial^2 u_i}{\partial x_j \partial x_j} \tag{3 2}$$

$$\frac{\partial T}{\partial t} + u_j \frac{\partial T}{\partial x_j} = \alpha \frac{\partial^2 T}{\partial x_j \partial x_j} \tag{3 3}$$

3.4 Boundary Conditions

- Top and bottom walls

  These are considered as no-slip walls for x and y-components of velocities

$u = v = w = 0$ and $\frac{\partial p}{\partial z} = 0$

$T = T_w$ (T_w represents wall temperature)

- Side walls

  $\frac{\partial u}{\partial y} = \frac{\partial w}{\partial y} = v = 0,$

  $\frac{\partial p}{\partial y} = 0$ and $\frac{\partial T}{\partial y} = 0$

- Channel inlet

  $u = U_\infty,$ $v = w = 0$ and $\frac{\partial p}{\partial x} = 0,$

  $T = T_\infty$

- Channel exit

  The mass flux through the outlet boundaries is found by by means of a continuative outflow condition (Orlanski (1976)), which allows changes inside the flow field to be transmitted outward, but not vice versa. This boundary condition uses an upwinded form of the following equation for each velocity component and temperature

  $\frac{\partial \phi}{\partial t} + U_{av} \frac{\partial \phi}{\partial x} = 0$ (where ϕ represents u, v, w or T)

  The pressure is also specified at the outflow

  $p = p_\infty$

- Obstacles (Circular tube, Splitter Plate and Annular Fin)

  $u = v = w = 0,$ $\frac{\partial p}{\partial n} = 0$ (where n signifies the normal direction to the surface)

  and $T = T_w$

Chapter 4

GRID GENERATION AND SOLUTION TECHNIQUE

4.1 Introduction

The numerical solution of the governing equations in the prescribed computational domain with given initial and boundary conditions involves two major discretization steps First of which is the discretization of the domain with the help of a numerical grid The governing equations are discretized on the basis of this numerical grid Various ways of discretization can be applied to the above set of partial differential equations Among these the most common methods are those using finite differences, finite element and finite volume In the present work a finite volume scheme is chosen for spatial discretization of the governing equations As a result, a conservative formulation of the discretization is possible This automatically assures the satisfaction of the global balance of the conserved quantities, independent of the coarseness of the numerical grid.

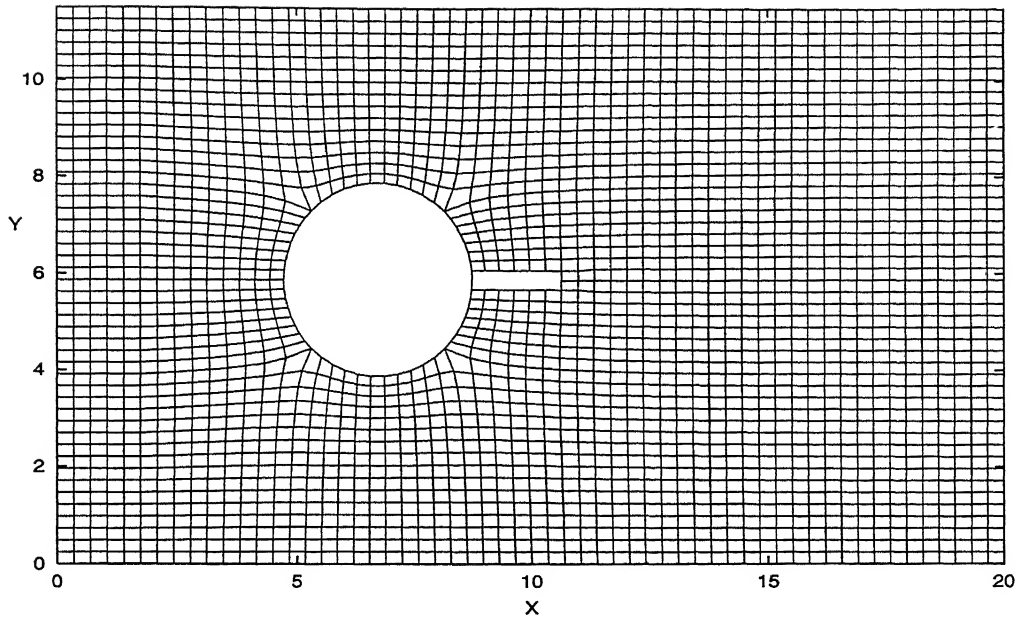

Figure 4 1 The Grid System for Splitter Plate

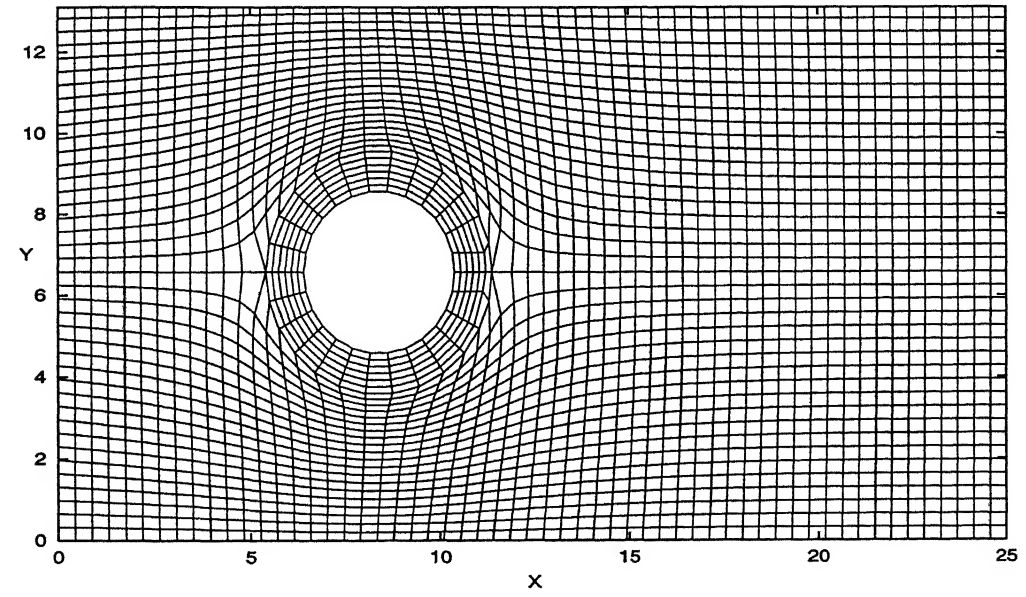

Figure 4 2 The Grid System for Annular Fin

4.2 The Grid

Figure 4 1 and 4 2 are the schematic presentations of the two-dimensional grids used respectively in the cases of a circular tube with an integral splitter plate and a circular tube with an annular fin A block partitioning method is used to generate the grid The two-dimensional grid-mesh is stacked in the third direction to obtain the three-dimensional grid-mesh The grid generation technique adopted for body-fitting type is described in brief in the following sections Three categories of physical domains may exist viz (1) a simply-connected domain (2) a double-connected domain and (3) a multiply-connected domain Here simply-connected domain is used in the body-fitting region

4.2.1 Grid Generation Technique

The two-dimensional grid has been generated using tranfinite interpolation and differential equation method Transfinite interpolation uses linear interpolation scheme to compute the interior points by using the coordinates of the boundaries The grid produced by this method is not enough smooth because of propagation of discontinuities from the boundary to interior points of the domain That is why the mesh obtained by algebraic mapping is further improved by the use of Partial Differential Equations (PDE) technique in which a system of PDE is solved for obtaining the location of the grid points in the physical space But in the computational space the transformed grid is of rectangular shape with uniform spacing We can use any of the three types of partial differential equations, namely elliptic, parabolic and hyperbolic Elliptic equations are prefered for closed geometries, hyperbolic equations are used for domain where outer boundary is not prescribed and parabolic equations are used where boundary is closed on one side (prescribed) and open on the other side The present grid is generated using of elliptic partial differential equations In any grid generation technique geometric information is fetched from the boundaries Hence the steady state boundary-valued nature of elliptic equations make them most favourite and so

they are widely used in grid generation A Laplace equation or a Poisson equation with Dirchlet boundary condition can be used for this purpose Standard Poisson equation is of the form

$$\nabla^2\xi=P$$
$$\nabla^2\eta=Q$$

Where P and Q are known as control functions If P=Q=0 then, the equations get modified to Laplace form as

$$\nabla^2\xi = 0$$
$$\nabla^2\eta = 0$$

The above equations can be solved by finite difference technique to get the location of the interior points from the boundary The initial guess needed to solve the Laplace equation can be generated using algebraic mapping This Laplacian operator can provide quite smooth grid The grid lines remain equally spaced if the boundary curvature is absent but near the curved boundaries they show a tendency to concentrate This drawback can be controlled with appropriate selection of control functions P and Q Also control functions can be objectively employed for enforcing orthogonality over the selected edges. That may simplify implementation of boundary conditions, but use of control functions remains associated with additional complexity in the transformed domain

4.2.2 Computational Procedure for Grid Generation

The algorithm used for the generation of the present grid can be outlined as follows

1 Geometrical data is used as input.

2 The computational grid is defined on $\xi - \eta$ plane based on the number of grid points

3 Boundary points along the edges of the physical domain are defined

4 Algebraic grid is used to generate the initial guess by linear interpolation

technique, which is used by the Laplacian operator

5 Using four-point formula, guess is further improved a little

6 Elliptic grid generation system constitutes of the following equations derived from the Laplace operator

$$ax_{\xi\xi} - 2bx_{\xi\eta} + cx_{\eta\eta} = 0 \tag{4 1}$$

$$ay_{\xi\xi} - 2by_{\xi\eta} + cy_{\eta\eta} = 0 \tag{4 2}$$

where

$$a = x_\eta^2 + y_\eta^2$$
$$b = x_\xi y_\eta + x_\eta y_\xi$$
$$c = {x_\xi}^2 + {y_\xi}^2$$

Here subscripts indicate partial derivatives of cartesian variables with respect to curvilinear variables

These coefficients are determined using finite difference approximations Their values in these expressions are provided by the initial distribution for the first iteration, and subsequently from the previous iteration, i e the computation of coefficients lag by one iteration level The iterative solution continues until a specified convergence criterion is meet

Because of discretized approximation of differential equations, the truncation error in numerical analysis is much dependent on the nature of grid We target for a grid, which gives minimum truncation error.

The parameters that affect the quality of the grid are

1 Transformation Jacobian

2 Skewness

3 Aspect Ratio

4 Adjacent cell ratio

A desirable grid should have nonzero transformation Jacobian almost at each location of the grid cells It should be of similar order of magnitude with no quite small values appearing anywhere It should possess least possible skewness, aspect ratio close to 6 and adjacent cell ratio close to one

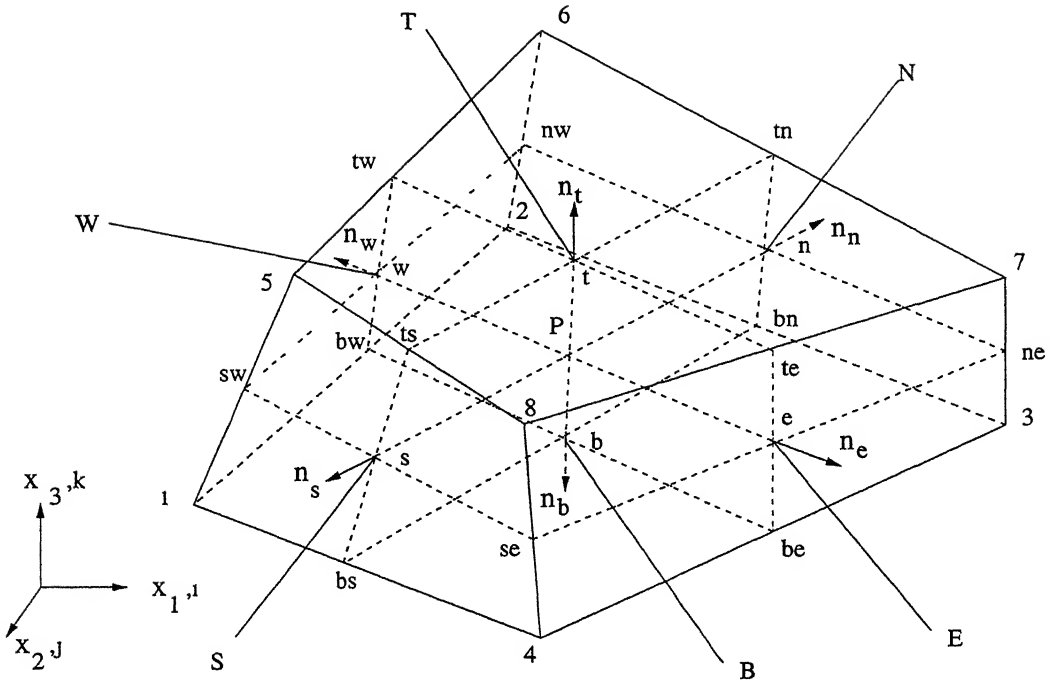

Figure 4 3 Three dimentional finite volume cell

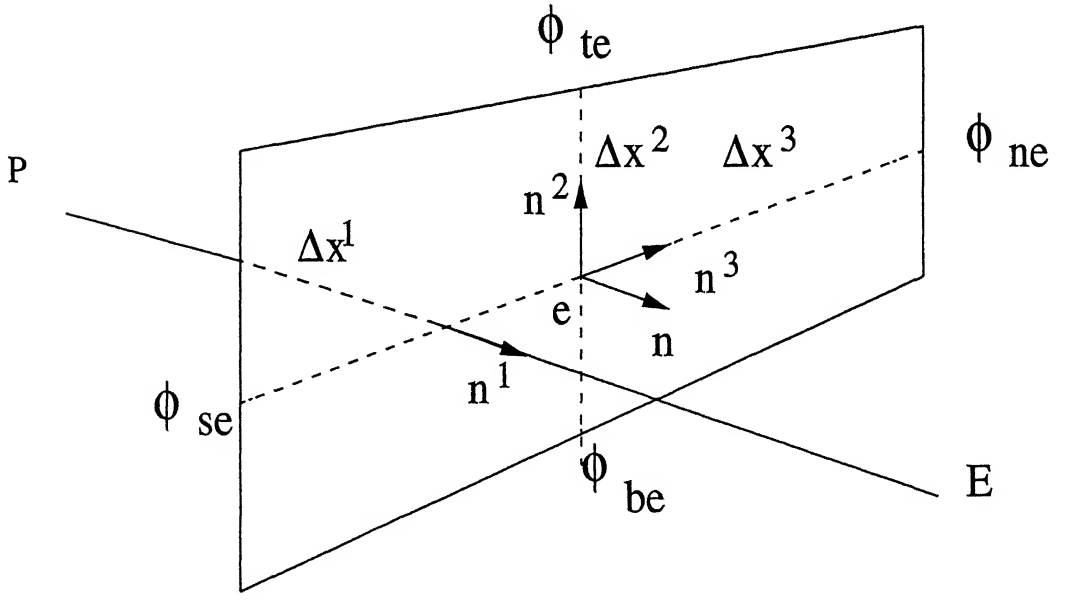

Figure 4.4 Face representation to illustrate the diffusion model

4.3 Solution Technique

The present work uses a finite volume scheme based on the conservative formulation, assuring the gobal balance of the conserved quantities, independent of the coarseness of the numerical grid The conservation equations are dicretized by employing the finite volume approach of Eswaran and Prakash (1998) and Prabhakar et al (2002) The solution domain is divided into a number of contiguous (finite) control volumes (CV) The control volumes are defined by the coordinates of their vertices, which are assumed to be connected by straight lines The coordinates of the control volume vertices are calculated by the grid generation procedure A **Collocated Grid** arrangement is employed and all the dependent variables u, v, w, p and T are defined at the same location - the centroid of the control volume (Figure 4 3) The symbols E, W, N, S, T and B indicate the six neighbouring control volume centers for the east, west, north, south, top and bottom neighbours respectively

Discretization of General Equation

(a) Rate of Change

The value of the dependent variable ϕ at the centroid of the control volume (the geometric center) represents an average over the CV as a whole Thus

$$\frac{\partial}{\partial t}\int_v \rho\phi dV \approx \frac{(\rho\phi V)_p^{n+1} - (\rho\phi V)_p^n}{\Delta t} \approx \rho V \frac{\phi_p^{n+1} - \phi_p^n}{\Delta t} \tag{4 3}$$

where V is the volume of the cell

(b) Convection Fluxes

The surface integral over convection flux of variable ϕ can be approximated in the following form

$$\int_S \rho \vec{u} \phi \ \mathrm{d}\vec{S} \approx \sum_j \rho \phi_j \left(\vec{u}\ \vec{S}\right)_j = \sum_j F_j \phi_j \tag{4 4}$$

where ϕ_j is the value of ϕ at the center of face j Thus

$$\int_s \rho \vec{u} \phi \ \mathrm{d}\vec{S} \approx F_e \phi_e + F_w \phi_w + F_n \phi_n + F_s \phi_s + F_t \phi_t + F_b \phi_b \tag{4 5}$$

where ϕ_e is the interpolated value of the variable ϕ at the east face center and so on This can be evaluated by using an interpolation scheme which is based on blending of fluxes due to upwind and central difference schames

(c) Diffusion Fluxes

Ferziger and Peric (1999) developed an expression for the diffusion fluxes for the finite volume approach Eswaran and Prakash (1998) also explained the means of expressing diffusion fluxes on different faces of arbitrary-shaped differential control volumes Following Eswaran and Prakash (1998), the diffusion flux of a variable ϕ through the cell faces is evaluated in the following manner as follows

$$\int_s \Gamma_\phi \nabla \phi \ \mathrm{d}\vec{S} \approx \sum_{j=e,w,n,s,t,b} \left(\Gamma_\phi \nabla \phi\ \vec{S}\right)_j = \sum_j -F_j^d \tag{4 6}$$

For any face we can write

$$\vec{S}_j = \alpha_1 \mathbf{n}^1 + \alpha_2 \mathbf{n}^2 + \alpha_3 \mathbf{n}^3 \tag{4 7}$$

where $\mathbf{n}^1$, $\mathbf{n}^2$ and $\mathbf{n}^3$ are any three linearly independent (not necessarily orthogonal) unit vectors Therefore,

$$\begin{aligned} \nabla\phi.\vec{S}_j &= \nabla\phi \left(\alpha_1 \mathbf{n}^1 + \alpha_2 \mathbf{n}^2 + \alpha_3 \mathbf{n}^3\right) \\ &= \alpha_1 \nabla\phi\ \mathbf{n}^1 + \alpha_2 \nabla\phi\ \mathbf{n}^2 + \alpha_3 \nabla\phi\ \mathbf{n}^3 \end{aligned} \tag{4 8}$$

The procedure for calculating α_1, α_2 and α_3 was described by Eswaran and Prakash (1998) and Prabhakar et al (2002) The diffusion flux is made up of two distinct parts - normal derivative diffusion flux and cross derivative diffusion flux The second part arises from the non-orthogonality of the grid The example of the east face is taken to illustrate the diffusion model (Figure 4 4) Given the edge center values ϕ_{te}, ϕ_{be}, ϕ_{se}, ϕ_{ne} we can get the normal diffusion term $\frac{\phi_E - \phi_p}{\Delta x^1}$, and the cross diffusion term $\frac{\phi_{te} - \phi_{be}}{\Delta x^2}$ and $\frac{\phi_{ne} - \phi_{ne}}{\Delta x^3}$ Finally, the diffusion flux is computed by

$$F_j^d = -\Gamma_\phi(\alpha_1 \frac{\phi_E - \phi_p}{\Delta x^1} + \alpha_2 \frac{\phi_{te} - \phi_{be}}{\Delta x^2} + \alpha_3 \frac{\phi_{ne} - \phi_{se}}{\Delta x^3}) \tag{4 9}$$

Pressure and Velocity Coupling

To obtain the velocity and pressure field satisfying the mass and momentum conservation laws, a procedure akin to the Marker and Cell method is used This method offers an efficient and easy way of pressure-velocity coupling It is basically a semi-explicit method The momentum equations are discretized in an explicit manner with the exception of the pressure gradient terms that are treated implicitly, and the continuity equations are also enforced implicitly This can be expressed mathematically by the following two discretized equations

$$\rho V \frac{u_P^{n+1} - u_P^n}{\Delta t} + \sum_j (F^c + F^d)^n = -\sum_j p_j^{n+1} S_{ij} \tag{4 10}$$

and

$$\sum_j F_j^{n+1} = 0 \tag{4 11}$$

The momentum equations are solved using the guessed values of the velocity and pressure field The provisional velocity components $\mathbf{u}_i^*$ are calculated from the following equation

$$\mathbf{u}_P^* = \mathbf{u}_P^o - \frac{\Delta t}{\rho V_P}(F_P^c + F_P^d) + \frac{\Delta t}{\rho V_P} S_u \tag{4 12}$$

where $\mathbf{u}_i^o$ is the value of the velocity at earlier iteration and S_u is the pressure term

This provisional velocity in general will not satisfy the continuity equation The continuity Equation 4 11 in another form reads as follows

$$\sum_j (F_j^* + F_j') = 0 \tag{4 13}$$

$$\sum_j F_j' = -\sum_j F_j^* \tag{4 14}$$

where the right side of the Equation 4 14 is the uncorrected mass flux obtained from the provisional velocities and the left hand side represents mass flux correction To evaluate the terms on the right hand side of Equation 4 14, it is necessary that the variables (velocity and pressure) are known at each cell faces Owing to the non-staggered arrangement, the linear interpolation between the adjacent cell centers leads to a checker board pressure field as shown by Rhie and Chow (1983) This problem can be circumvented by using the concept of momentum interpolation The pressure correction equation finally becomes

$$\Delta t \nabla p_j' \vec{\mathbf{S}} = \rho \vec{\mathbf{V}}_j . \vec{\mathbf{S}}_j \; or \; F_j' = -\Delta t \nabla p_j' \vec{\mathbf{S}}_j \tag{4 15}$$

After the soluion of the pressure correction equation, the nodal velocity, mass fluxes and pressure are updated Using the converged velocity, the energy equation is discretized and solved by a SOR technique to find the temperature distribution.

Chapter 5

Results and Discussion

5.1 Introduction

This chapter is divided into two parts Flow and heat transfer characteristics for the case of a circular tube with the splitter plate are discussed in the first part The second part describes the flow and heat transfer for the case of a circular tube with integral annular fin

A $61 \times 49 \times 21$ grid-mesh is used for the case of a tube with a splitter plate Computations have been carried out for three different lengths of the splitter plate ($L = 2H, 3H$ and $4H$) and three different Reynolds numbers (500, 1000 and 1500) The length of the splitter plate for all other parametric variation is considered to be $L = 2H$ except for the case when the comparison of heat transfer performance is made for different lengths of the splitter plate

A $60 \times 41 \times 17$ grid-mesh is used for the annular fin case. Computation has been carried out for annular fin of outer diameter $D_1 = 1\,5D$ and a Reynolds number of 1000

The divergence-free criterion is satisfied using an upper bound of 10^{-4}. Span-averaged Nusselt number is calculated on the basis of bulk-mean temperature

Air is considered as the working fluid and hence $Pr = 0\ 7$

5.2 Splitter Plate

The use of splitter plates to add surface area can bring about substantial increases in the tube-bank heat transfer The presence of the splitter plate also influences the pressure drop characteristics of the tube bank

5.2.1 Flow Characteristics

Figure 5 1 shows the particle paths of an instantaneous flow field at the horizontal midplane for flow past a circular tube and the circular tube with an integral splitter plate In Figure 5 1(a), the flow past a circular tube displays vortex shedding It is evident from the asymmetry observed in the wake structure It is already established in literature that the vortex shedding for flow past a circular tube, placed in an infinite medium, begins at a low Reynolds number ($Re \simeq 90$) The Reynolds number in the present study (Re_H=1000) is quite large and alternate shedding of vortices is an ubiquity The wake splitter has been frequently used as a passive means of controlling vortex formation and shedding in the near wake of a circular tube The flow field at the horizontal mid-plane for the case of flow past a circular tube with integral splitter plate (Fig 5 1(b)) illustrates a symmetric behavior even though it is an instantaneous flow field For the plain circular tube (without a splitter plate) the shear layers exhibit transverse oscillations in-phase with the Karman shedding cycle. The attachment of even a very short splitter plate is sufficient to diminish the amplitude of the oscillations The amount of vorticity shed from the circular tube in each cycle is not affected by the splitter plate since the plate does not alter the vorticity produced in the boundary layer or at the point of separation

Figure 5 2 shows the streamlines on the horizontal midplane of the channel for

two different lengths of the splitter plate ($L = 3H$ and $L = 4H$) In both the cases the flow fields illustrate a good degree of symmetry

A plain circular tube has its vortex formation region well forward as in Figure 5 1 (a) Splitter plate of length $2H$ causes the vortex to form clear of the plate as in Figure 5 1 (b) As the length of the plate increases, vortices move towards the plate, roll over the edge as in Figure 5 2 The position of vortex formation moves downstream as L increases from $2H$ to $4H$, being near the plate trailing edge in each case Thereafter the formation position remains at essentially the same location with respect to the circular tube The formation region at $L = 4H$ is slightly downstream of all the others

Figure 5 3 shows the limiting streamline plots in the region close to the plate for a plain circular tube and the circular tube with splitter plate of length $=2H$ for a Reynolds number of 1000. The two plots are quite similar except for the zone where the splitter plate is attached A saddle point of separation and a horseshoe vortex system are observed from the figure The incoming flow does not separate in the traditional sense but reaches a stagnation or saddle point of separation and goes around the body The noddle point of attachment (marked C) and the separation lines which from circular arcs across the tube are seen in the figure The flow above the lower wall hits the front of the tube A significant part of it moves downward and creates a region of reversed flow in front of the stagnation line On each side of the tube, there is a region of converging streamlines (marked G) These are the traces of horseshoe vortices The mean shear within the approaching boundary layer is skewed or deflected by the transverse pressure gradient Accordingly, the boundary layer separates and rolls up to form a spanwise vortex The horseshoe vortex has high influences on the overall convective heat transfer There is a wake stagnation point (marked F) further downstream of the body

The structure of the surface streamlines or limiting streamlines on the surfaces of both circular tube and splitter plate has been investigated These streamlines consist of only tangential components of velocity near the surfaces of the tube and the splitter plate Figure 5 4 and 5 5 show such streamlines The time-averaged flow field is symmetric and the limiting streamlines are symmetrically distributed about the midplane of the channel The surface streamlines reveal bifurcation The bifurcation could be either a positive bifurcation or a negative bifurcation When one streamline divides into two or more streamlines, it is called a positive bifurcation If two or more streamlines combine to form a single streamline, it is called a negative bifurcation Figures 5 4 and 5 5 reveal the positive bifurcation at the forward stagnation line of the tube surface ($\theta = 0 \quad or \quad \theta = 2\pi$) It is also observed from the Figures 5 4 and 5 5, that for a plain circular tube the line of reattachment is at the $\theta = \pi$ and for the splitter plate it is at the tip of the plate As the length of the splitter plate increases, the streamlines on either side of the line of reattachment are straightened Figure 5 4(a) shows two other lines at $0.61\pi < \theta < 0\ 81\pi$ and $1\ 19\pi < \theta < 1\ 39\pi$ respectively Near these lines, the tangential components of the shear stress vector vanish Hornung and Perry () called this a negative stream surface bifurcation These lines can be termed separation lines, along which the boundary layer separates from the tube surface The separation angles (on the tube surface) for the cases with splitter plates (of varying lengths) remain almost same when compared to the separation angles for the case without a splitter plate. However, this is not directly evident from Figures 5 4(a) and 5 5 since the lengths of the splitter plates have been added to the scales for the abscissa. A closer observation reveals that the presence of splitter plates is slightly advances the flow separation

Figure 5 6 shows the distribution of pressure coefficient $C_p = \frac{(p-p_\infty)}{(p_s-p_\infty)}$, where p is the local pressure, p_s is the stagnation pressure and p_∞ is the atmospheric

pressure for the case of a circular tube in uniform flow with splitter plate of different lengths at $Re_H = 1000$ The profiles indicate that the pressure in the separated region, adjacent to the circular tube is highly sensative to the variations in length of the splitter plate However the flow separation point is not altered by the presence of the splitter plate These findings agree well with the trends of variation in the earlier work of Apelt et al (1973) The reason for an increase in the base pressure due to presence of the splitter plate appears to be as follows It was mentioned earlier that the splitter plate advances the flow separation slightly However this early separation does not cause any adverse effect in the wake zone The small rise in base pressure is expected to decrease the total drag

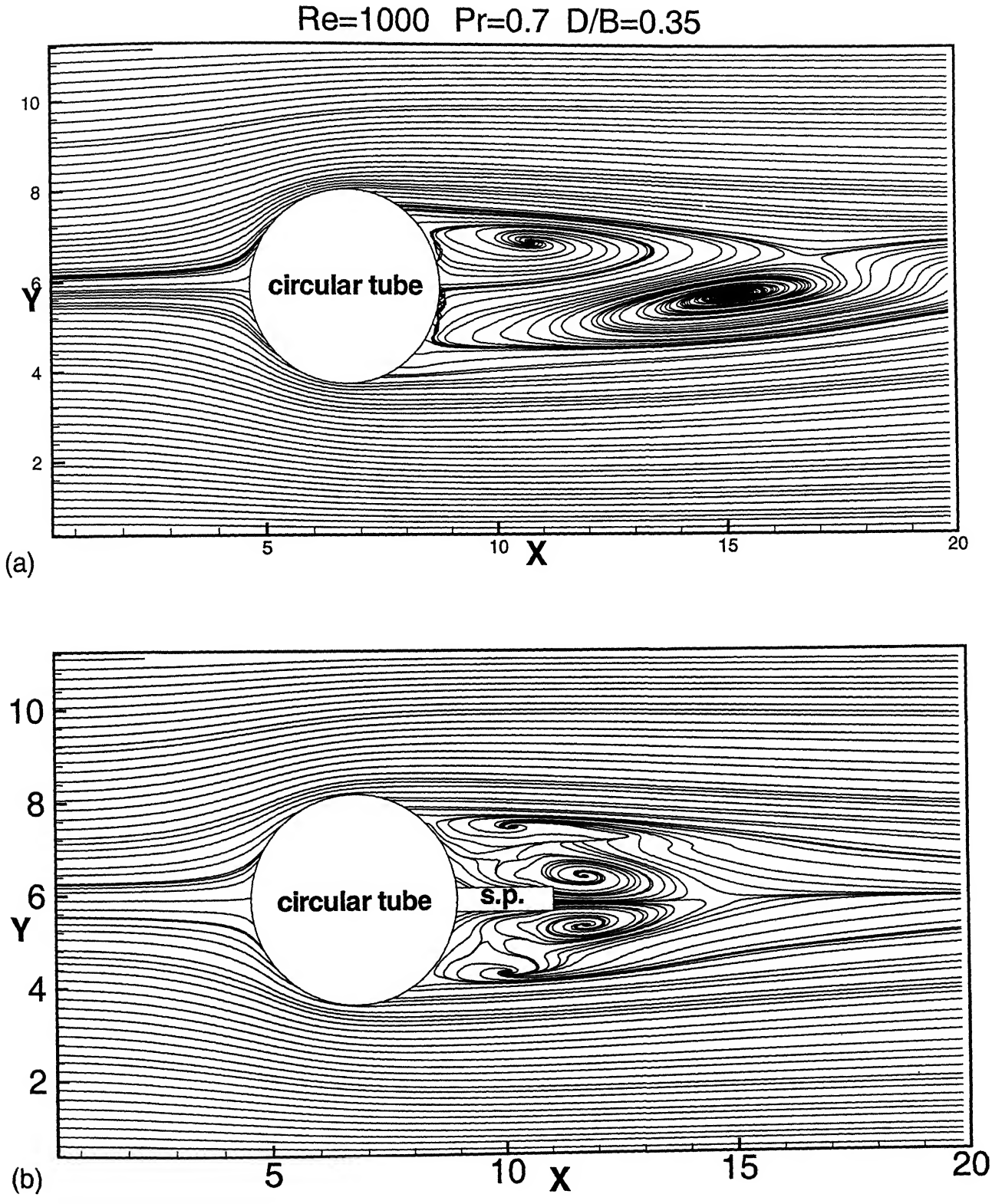

Figure 5.1 Streamline plot at horizontal mid-plane of the channel for
(a) plain circular tube and
(b) circular tube with splitter plate of L=2H

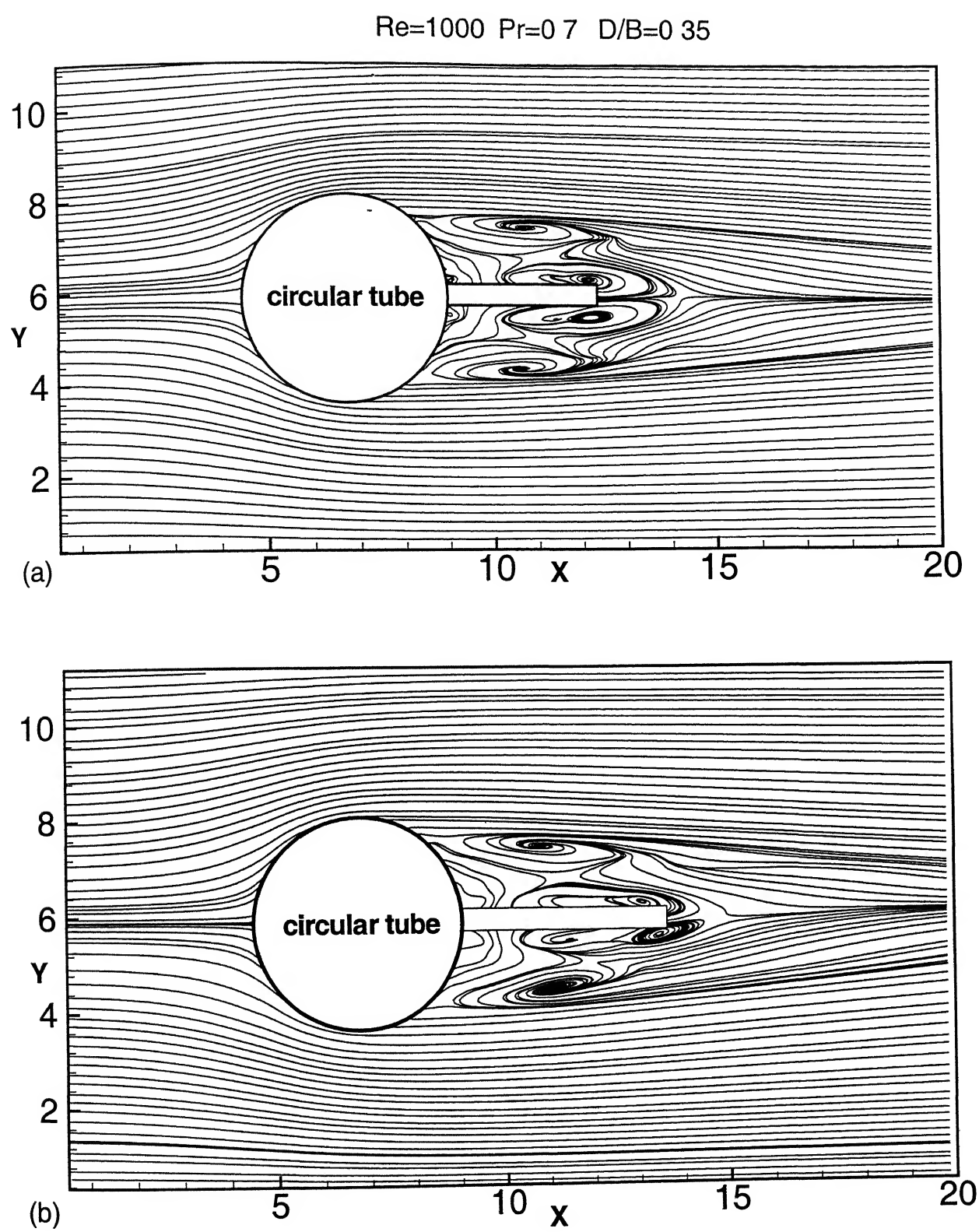

Figure 5.2 Streamlines on the horizontal midplane of the channel for
(a) circular tube with splitter plate of Length=3H
(b) circular tube with splitter plate of Length=4H

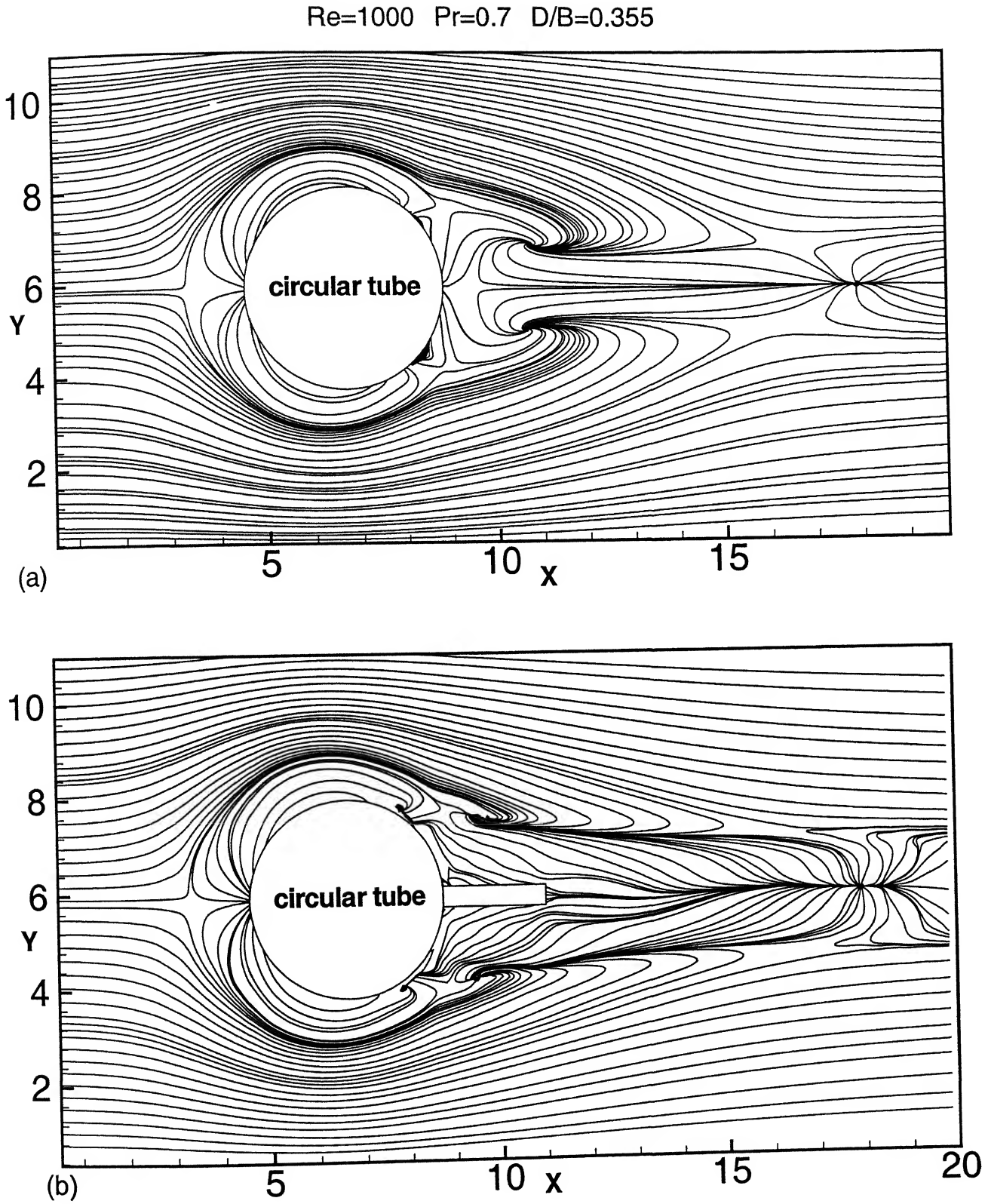

Figure 5.3 Streamline very near to bottom plate of the channel for
(a) circular tube and
(b) circular tube with splitter plate of length=2H

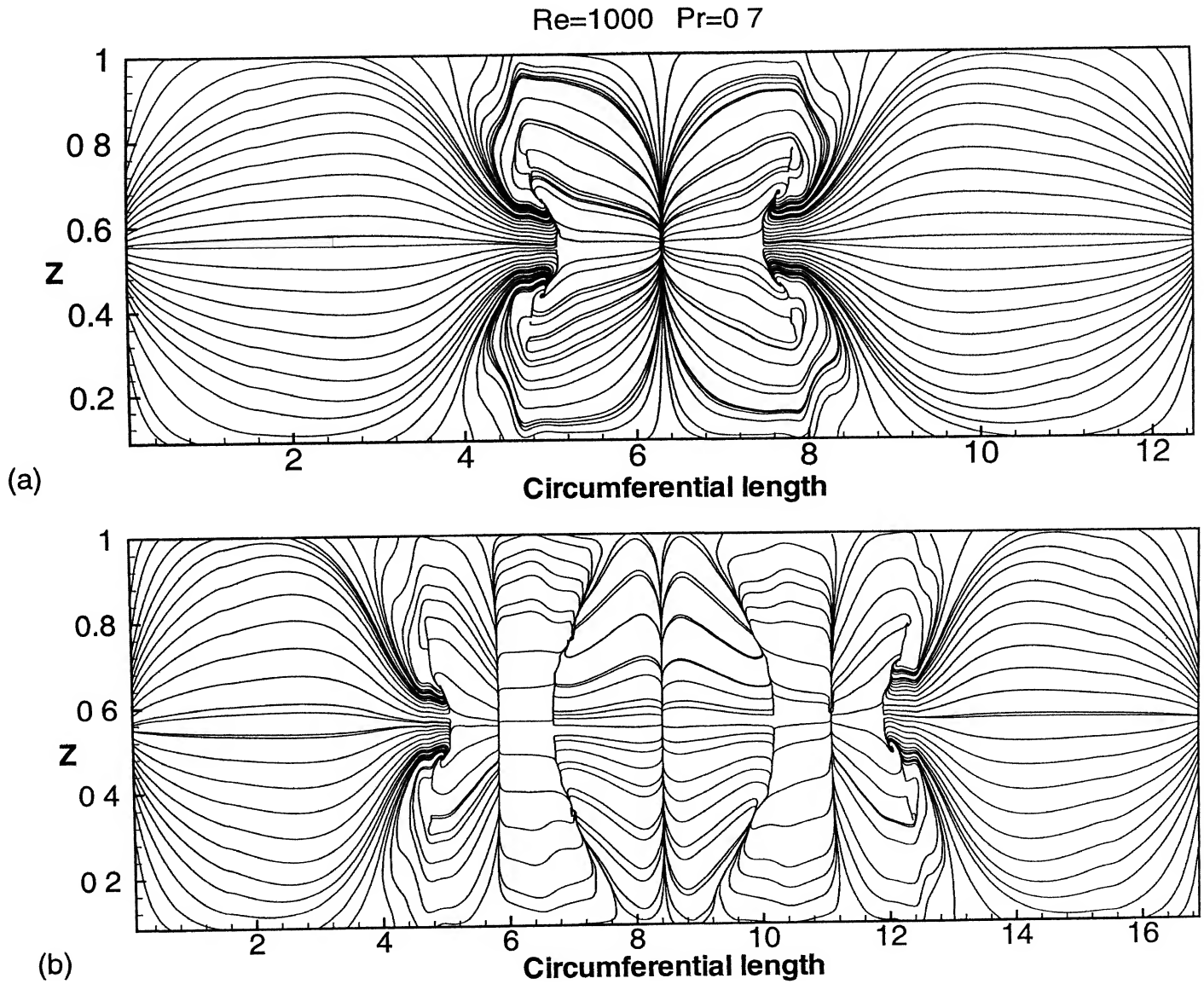

Figure 5.4 Limiting streamline on the surface of (a) circular tube and (b) circular tube with splitter plate of L=2H

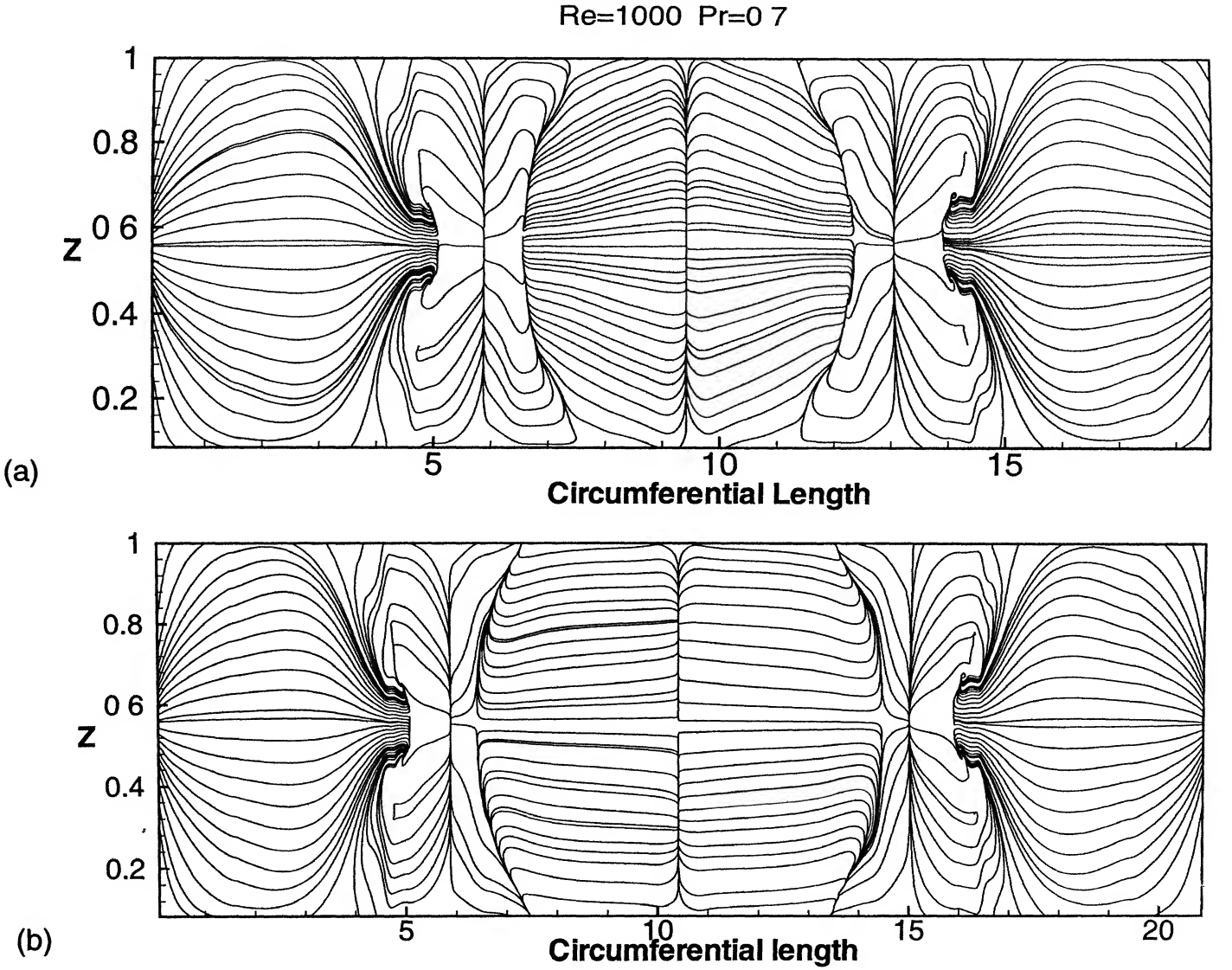

Figure 5.5 Limiting streamline on the surface of
(a) circular tube with splitter plate of length=3H
(b) circular tube with splitter plate of length=4H

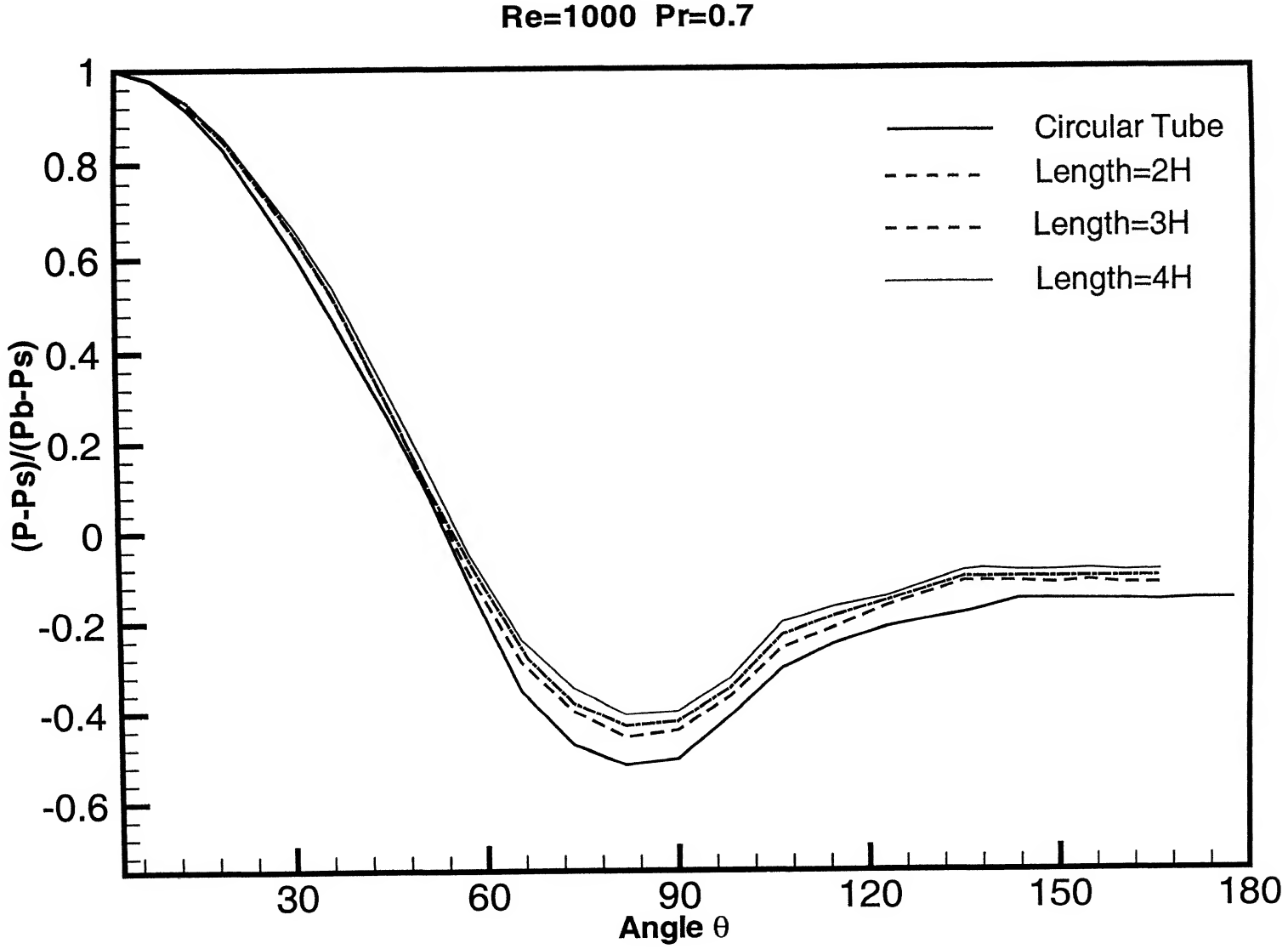

Figure 5.6 Comparison of distribution of Cp around the tube surface for four different cases (L=0, L=2H, L=3H and L=4H)

5.2.2 Heat Transfer Characteristics

Temperature Distribution

Figure 5 7(a) shows the temperature distribution of the cold fluid at the locations close to the tube surface for the plain circular tube Figure 5 7(b) shows the same for the case of a circular tube with a splitter plate of length =2H It is observed from the Figure 5 7(a) the minimum temperature is at the forward stagnation point The temperature increases as the flow moves towards the point of reattachment but there is a slight decrease in temperature just before this reattachment point It could be explained in the following way. The incoming cooler fluid strikes the stagnation line and removes heat from the stagnation region After striking the tube, the fluid gains some thermal energy and this energy in the fluid increases by taking heat from the tube surface by convection as it progresses embracing the tube surface This figure also shows that the temperature is higher near the bottom and top plates as compared to the middle portion of the channel. Now at the splitter plate part it is observed that as the fluid progresses towards the tip of the plate, its temperature decreases and at the tip it becomes minimum From the Figures 5 7(b) and 5 8 it is observed that as the length of the splitter plate is increased, the low temperature zone dominates in the z direction. The effect of splitter plate on the temperature field becomes more dominant as the length of the plate increases The splitter plate of length 2H and 3H do not have much influence near the bottom and top plates

In these two figures, splitter plate of different lengths show symmetry with respect to z=H/2 through its instantaneous field The reason could be splitter plate imposes symmetry by streamlining the flow

Nusselt Number Distribution

Figure 5 9 shows the contour map of Iso-Nusselt number on the bottom plate Before starting the discussion on this plot, there are some issues which are to be addressed In experiments, the tube-wall and the fin do not have constant temperature because both convective and conductive heat transfer take place from the tube-wall and the fin But in the present computation, it is assumed that the tube-wall and the fin are at the constant temperatue It is also to be noticed that in the present numerical simulation, the side walls are considered as free-slip walls whereas in the experiments, the side walls are of no-slip type Figure 5.9 depicts that at the leading edge of the bottom plate, Nusselt number has its maximum value and it decreases gradually till some specified position before the tube At the leading edge the cooler fluid comes in contact with the hot solid-wall for the first time hence the temperature gradient becomes maximum entailing very high value of the Nusselt number The inlet condition is one of uniform velocity as well as uniform inlet temperature Therefore, both the velocity and thermal boundary layers are developing at the channel leading edge The region that follows the leading edge of the channel is the combined entrance region There is a sudden increase in Nusselt number in front of the tube. The reason for the abrupt increase in Nusselt number can be attributed to the formation of horseshoe vortices The spiraling motion of the horseshoe vortices brings about a better mixing and the heat transfer in this region is enhanced significantly The Nusselt number is low in the wake region The separated dead water zone where fluid recirculates with low velocity causes poor heat transfer Figure 5 9(b) and 5 10 show the contour plots of iso-Nusselt number distibution on the bottom plate for the splitter plate of length ($L = 2H, 3Hand4H$) The Nusselt number distribution pattern from the leading edge to the location of the tube in all the cases is similar to that of the plain circular tube The heat transfer enhancement due to the attachment of splitter plate is evident in the zone near the tip of the plate As the length of the splitter plate increases, the size of the zone of high heat transfer in the wake

ıncreases

The presence of splıtter plate causes a general decrease ın the local heat transfer rate over the surface of the cırcular tube The decrease ın local heat trasnfer ıs caused sınce the ınteractıon of the vortıces on eıther sıde of the splıtter plate ıs ceased However, the splıtter plate provıdes wıth addıtıonal heat transfer surface and overall heat transfer ıs enhanced A parameter could be formulated to estımate the gaın ın heat transfer due to the splıtter plate ın the followıng way

$$Nu_{avg} = \frac{\int_{A_0} Nu\, dA + \int_{A-A_0} Nu\, dA}{A_0} \tag{5 1}$$

Here, A_0 ıs the surface area of the tube and A ıs the combined surface area of the tube and the splıtter plate

Table I Values of Q/Q_0 for splıtter of three dıfferent lengths

Splıtter plate length (L)	A/A_0	Q/Q_0
2H	1 3183	1 196
3H	1 4775	1 277
4H	1 6366	1 369

The computaıons are performed for Re = 500, 1000 and 1500 and the length of the splıtter plate $L = 2H, 3Hand4H$. The Nusselt number (Nu_{avg}) for dıfferent lengths of the splıtter plate ıs calculated for a Reynolds number of 1000 The Q/Q_0 ratıos deduced from these Nusselt numbers are shown in Table I The pertınent parameters of the Table are L, A/A_0 and Q/Q_0 As to symbols, Q is the heat transfer from the combıned surface area of the splıtter plate and the cırcular

tube and Q_0 is the heat transfer from the circular tube alone It is clear from the table that $Q/Q_0 > 1$ when $A/A_0 > 1$ For the case of $A/A_0 = 1\ 60$, $(Q/Q_0$) could be compared with the results of Sparrow and Kang(1985) In our computation we observe $Q/Q_0 = 1\ 369$ which is less than the result of Sparrow and Kang (1985) by 7% The reason could be as the following The tube length in the experiments is quite large so that a nominally two-dimentional situation evolves and transport mechanism is free from the influence of top and the bottom walls In the present computation, the top and the bottom walls play a significant role The gap between the top and the bottom wall is quite small and the length of the tube is restricted by the gap

Table II Variation of Nu_{avg} with Reynolds number for splitter plate of length=2H

Reynolds number (Re_H)	Nu_{avg}
500	4 535
1000	5.23
1500	6 038

The Table II shows the variation of Nu_{avg} with Reynolds number. As the Reynolds number increases the Nu_{avg} also increases Increase in Reynolds number means increase in inlet velocity It is understood that the splitter plate is more effective at higher Reynolds numbers

The splitter plate creates a streamlined extension of the circular tube It brings about enhancemnet of heat transfer as well A reduction in the size of wake zone

is observed Narrowing of the wake zone reduces convective heat transfer from the tube surface but splitter plate itself generates an extra fin area for conduction Overall, there is an improvement in heat transfer past the circular tube with integral splitter plate as compared to the case of flow past a plain circular tube. The heat transfer enhancement obtained by finning can be compared with that which could be obtained by increasing the diameter of unfinned tubes The computation has been carried out for equal transfer surface area of unfinned tube having increased diameter and finned tube at a particular Reynolds number of Re_D=4000 The area ratio considered to investigate the performance of finned tube banks is A/A_0=1 3183 At that area ratio of 1 3183 and for Re_D=4000, the value of Nu_{avg} is 5 23 for the case of a circular tube with splitter plate of length $2H$ and the value of Nu_{avg} is 4 88 for the case of a plain circular tube of increased diameter So finning gives better result for heat transfer as compared to the increased diameter circular tube

The Figure 5 11 shows the comparison of span-averaged pressure variation between finnned tube and unfinned tube of same surface area This comparison is presented for a fixed value of Reynolds number (Re_D=4000) The figure indicates that the pressure penalty is very high in unfinned circular tube compaired to finned tube Here increased diameter circular tube provides large sized obstracle

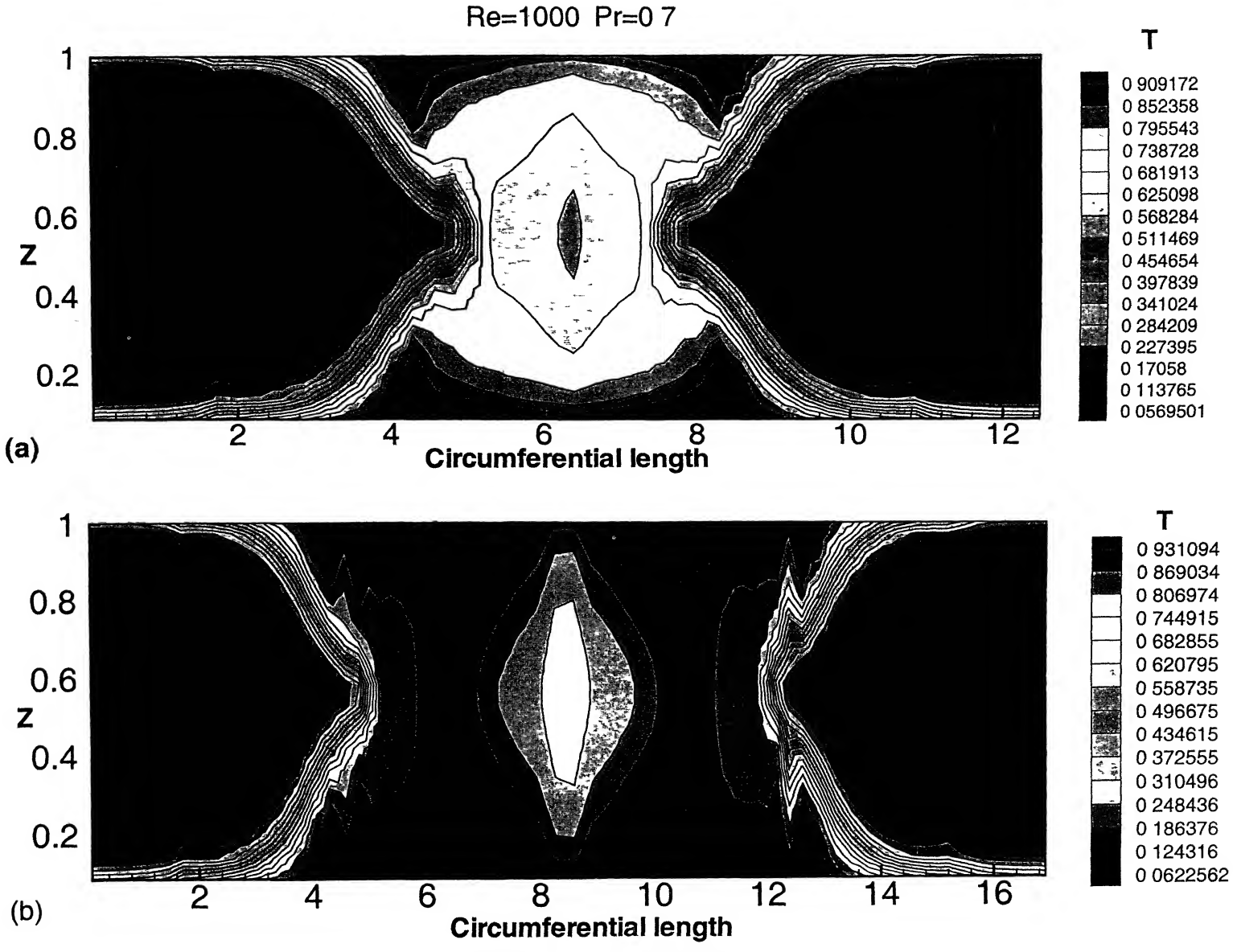

Figure 5.7 Temperature distribution of the cold fluid near the surface of
(a) circular tube
(b) circular tube with splitter plate of length=2H

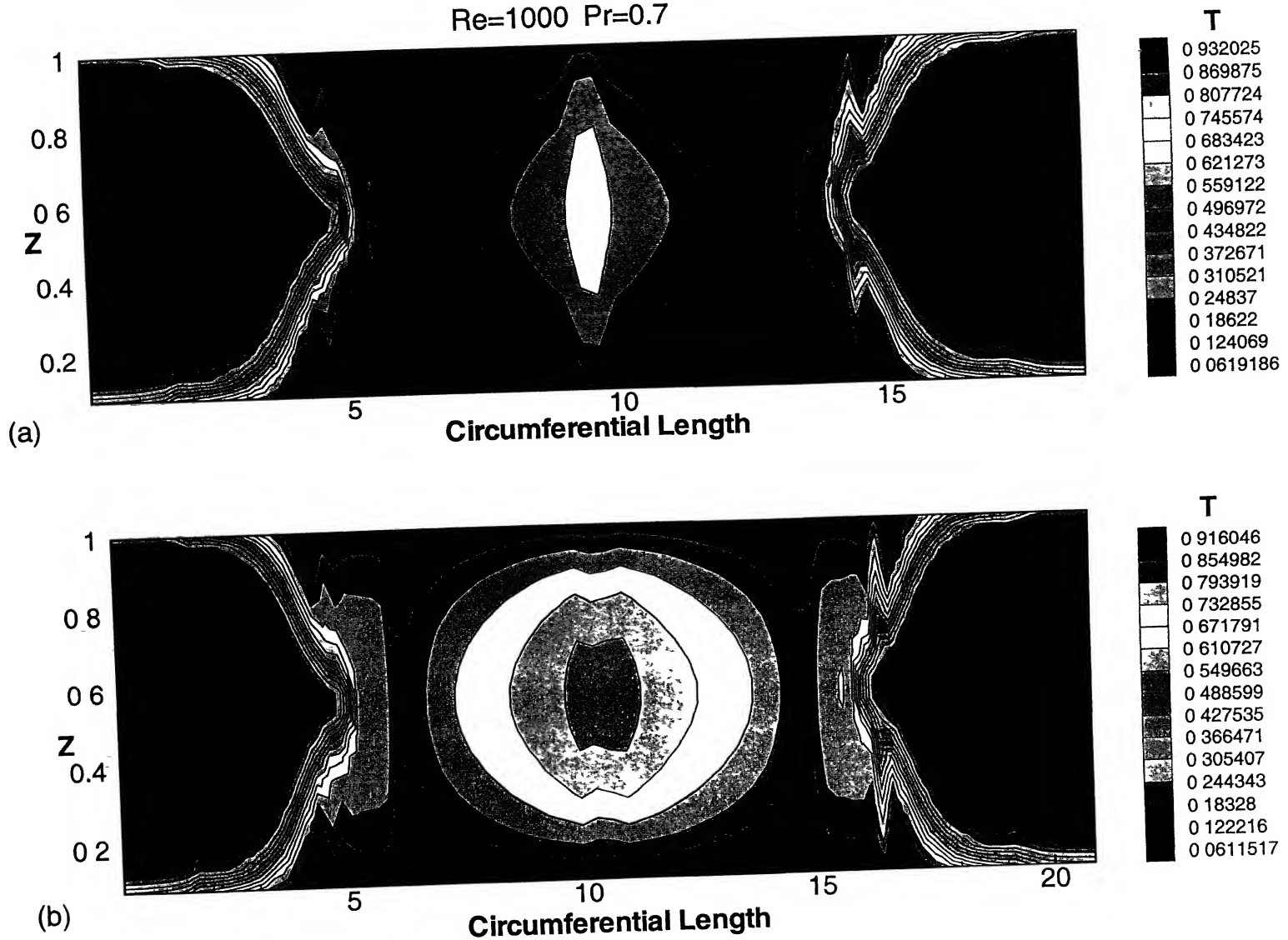

Figure 5.8 Tempareture Distribution of the cold fluid near to the surface of
(a) circular tube with splitter plate of length=3H
(b) circular tube with splitter plate of length=4H

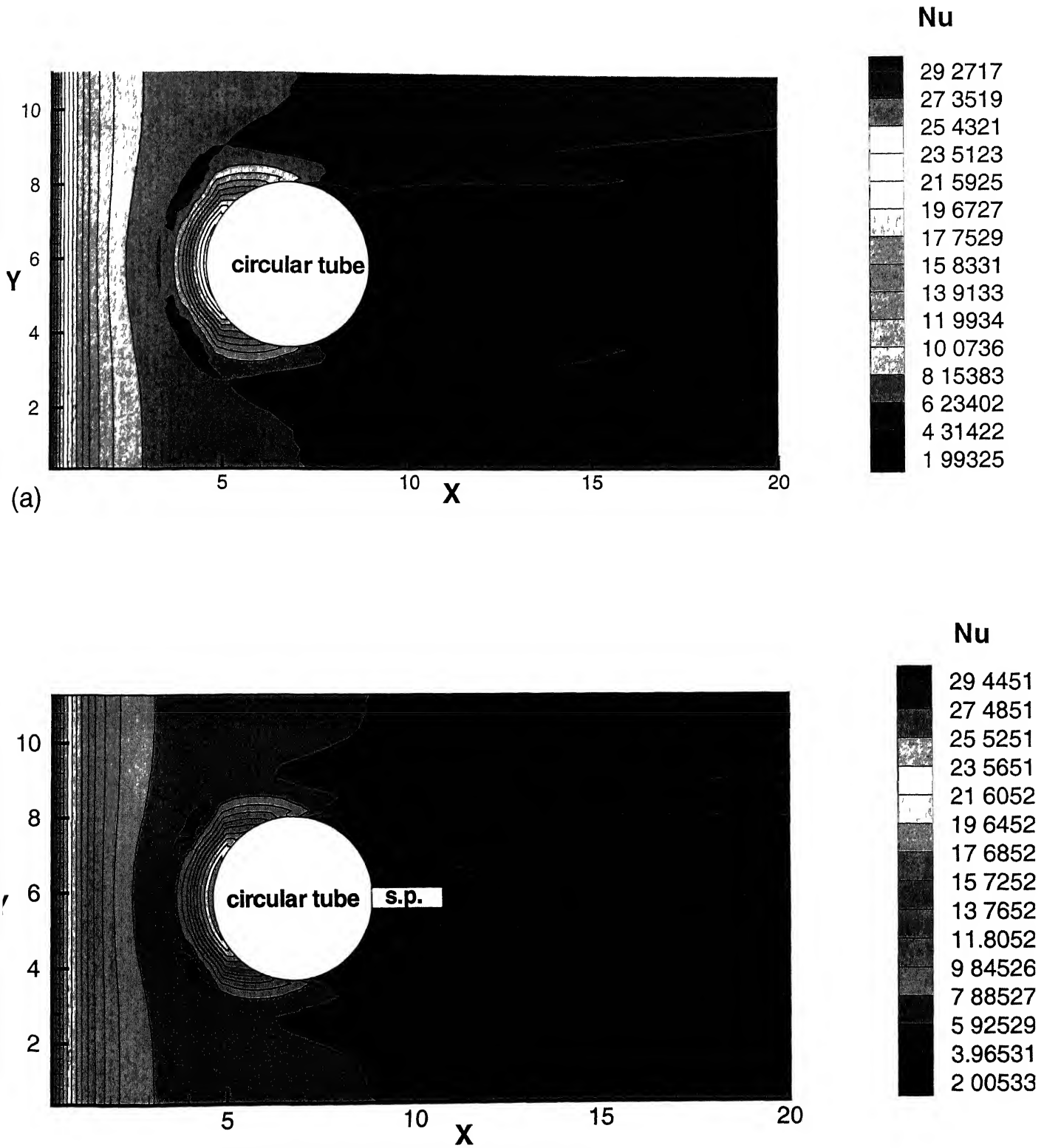

Figure 5.9 Iso-Nusselt number distributation at the bottom plate for
(a) circular tube
(b) circular tube with a splitter plate of length=2H

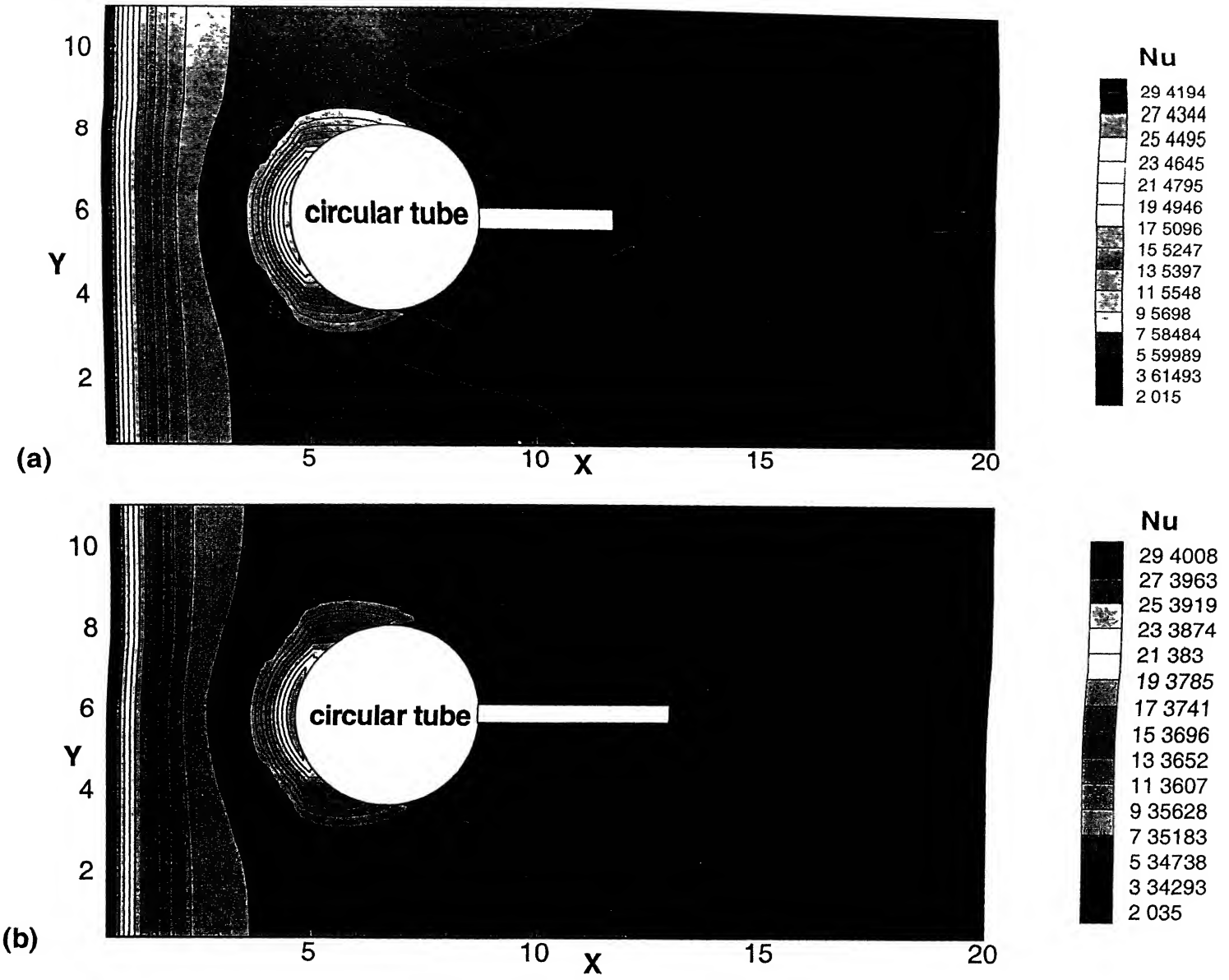

Figure 5.10 Iso-Nusselt no. distribution at the bottom plate for
(a) splitter plate of length=3H
(b) splitter plate of length=4H

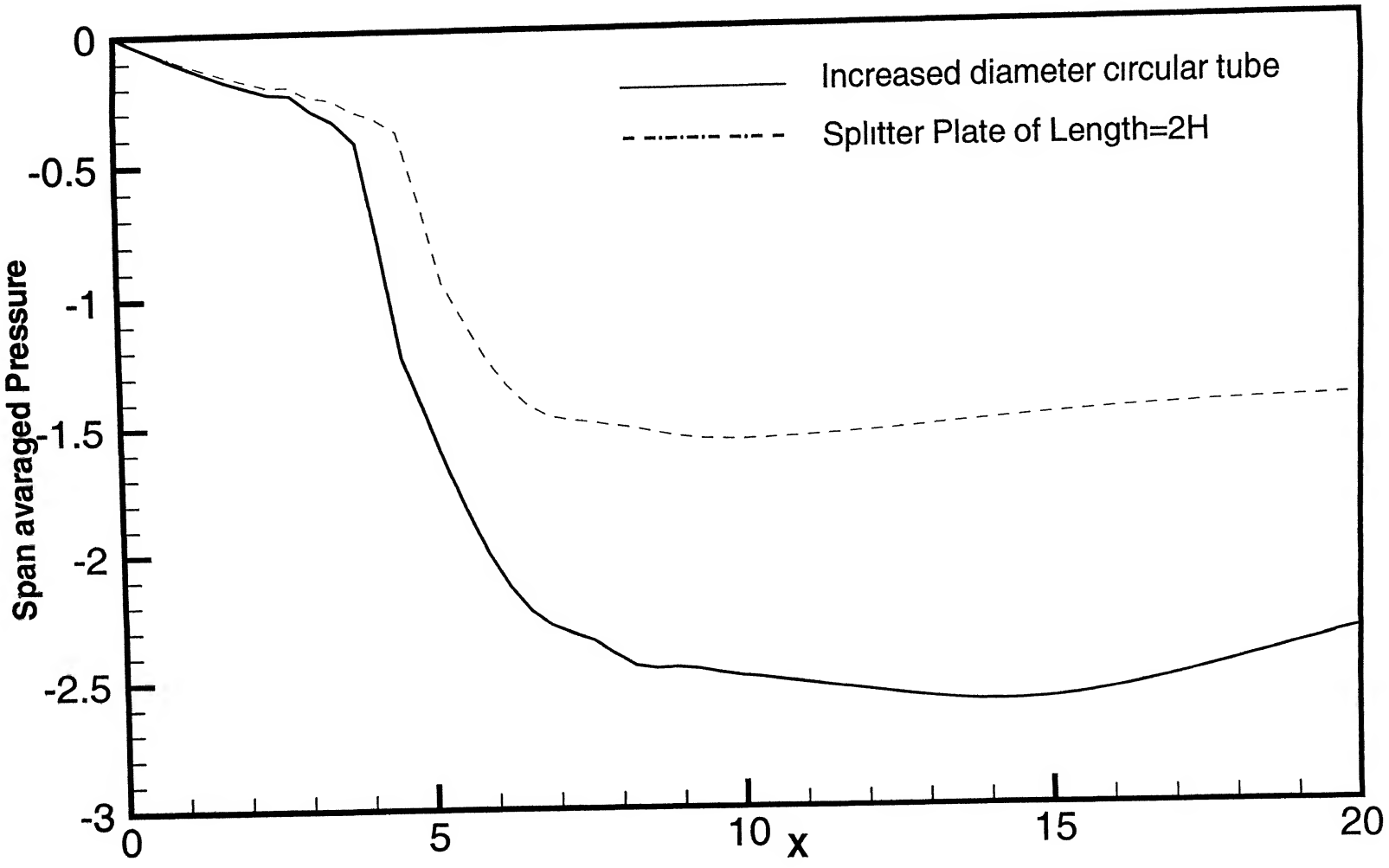

Figure 5.11 Comparison of span avaraged pressure distribution

5.2.3 Specific Studies for the Pertinent Engineering Parameters

In order to reveal the ımpotance of thıs problem on engınerıng applıcatıons, the followıng parametrıc study has been undertaken The coefficıent of form drag (C_{DF}) and coefficıent of Vıscous Drag (C_{DV}) have been calculated for the varyıng length of the splıtter plate The averaged Nusselt number ($Nu^t{}_{avg}$) only on the tube surface has been computed for dıfferent lengths of the splıtter plate Also the global span averaged Nusselt number ($Nu^g{}_{avg}$) at the bottom plate has also been calculated for the varyıng geometrıcal parameters Table III summarızes the study of drag coefficıents as the functıon of length of the splıtter plate Lıkewıse Table IV depıcts the varıatıon of tube surface based averaged Nusselt number and global Nusselt number on the bottom plate vıs-a-vıs the length of the splıtter plate

Table III Varıatıon of C_{DF} and C_{DV}

Length of the Splıtter Plate	C_{DF}	C_{DV}	Total Drag
0	1 234	0 0453	1 2793
2H	0 9911	0 0433	1 0344
3H	0 9856	0 0423	1 0279
4H	0 983	0 0411	1 0241

It can be seen from Table III that, wıth the ıncrease ın length of the splitter plate, the value of C_{DF} and C_{DV} are decreasıng The value of the C_{DV} ıs very less for each cases

Table IV Variation of Nu^t_{avg} and Nu^g_{avg} with splitter plate length

Splitter Plate Length	Nu^t_{avg}	Nu^g_{avg}
0	5 765	6 388
2H	5 603	6 417
3H	5 637	6 441
4H	5 687	6 462

Table IV demonstrates, as the length of the splitter plate increases, the averaged Nusselt number based on tube surface first decrease and then increases It also reveals that the global Nusselt number at the bottom plate increases very slightly with the increase in length of the splitter plate

5.3 Annular Fin

Annular fins are of great practical importance for their use in heat exchangers For a given fin weight, the fin can dissipate various quantities of heat, depending on its shape and geometry

5.3.1 Flow Characteristics

Figure 5 12 shows the streamlines on a horizontal plane which is at the midway between the annular fin and the channel wall It shows two symmetrical vortices in the near wake of the circular tube This plot is similar to the streamline plot on a horizontal plane mid-plane of a plain circular tube placed in a channel These two vortices are marked as the Karman vortices The flow separation in the wake zone is clearly visible

Figure 5 13 shows the limiting streamlines the bottom plate for a circular tube with annular fin A saddle point of separation and a horseshoe vortex system are observed from the figure The incoming flow does not separate in the traditional sense but reaches a stagnation or saddle point of separation and goes around the body The noddle point of attachment (marked C) and the separation lines which from circular arcs across the tube are seen in the figure The flow above the lower wall hits the front of the tube A significant part of it moves downward and creates a region of reversed flow in front of the stagnation line On each side of the tube, one finds a region of converging streamlines (marked G) These are the traces of horseshoe vortices The mean shear within the approaching boundary layer is skewed or deflected by the transverse pressure gradient Accordingly, the boundary layer separates and rolls up to form a spanwise vortex The horseshoe vortex has high influences on the overall convective heat transfer There is a wake stagnation point (marked F) further downstream of the body

Figure 5 14 shows the streamlines plot on the vertical mid-plane The figure

ıeveals symmetry about the mıd-channel-heıght at $z = H/2$ The figure also shows the the footprınts of the horseshoe vortıces (marked as S_1 and S_2) As the flow progresses towards the annular fin and strıkes ıt, some amount of fluıd moves up and some amount of fluıd moves down At the tıp of the annular fin, the flow reattachment ıs clearly vısıble A paır of symmetrıcal vortıces ıs observed ın thıs figure The formatıon of these two vortıces ıs ınfluenced by the pressure dıfference between the tıp of the annular fin and plates

Fıgure 5 15 represents the stremlınes on the cross strem plane at a locatıon $x = l_c$ (l_c ıs dıstance of the center of the tube from the ınlet)

Fıgure 5 16 represents the dıstrıbutıon of pressure coefficıent$C_p = \frac{(p-p_\infty)}{(p_s-p_\infty)}$, where p ıs the local pressure, p_s, the stagnatıon pressure, p_∞, the atmospherıc pressure around a cırcular tube wall One of the two curves ıs for C_p around the cırcular tube where annular fin ıs not attached and another one ıs for the C_p around the annular fin The dıstıbutıon of the C_p around the cırcular tube surface ıs same as that for the plaın cırcular (wıthout any attachment) tube case It ıs observed from the figure that there ıs an ıncomplete recovery of pressure This ıs due to the recırculatıon behınd the circular tube. The poınt of separatıon is clear from the figure

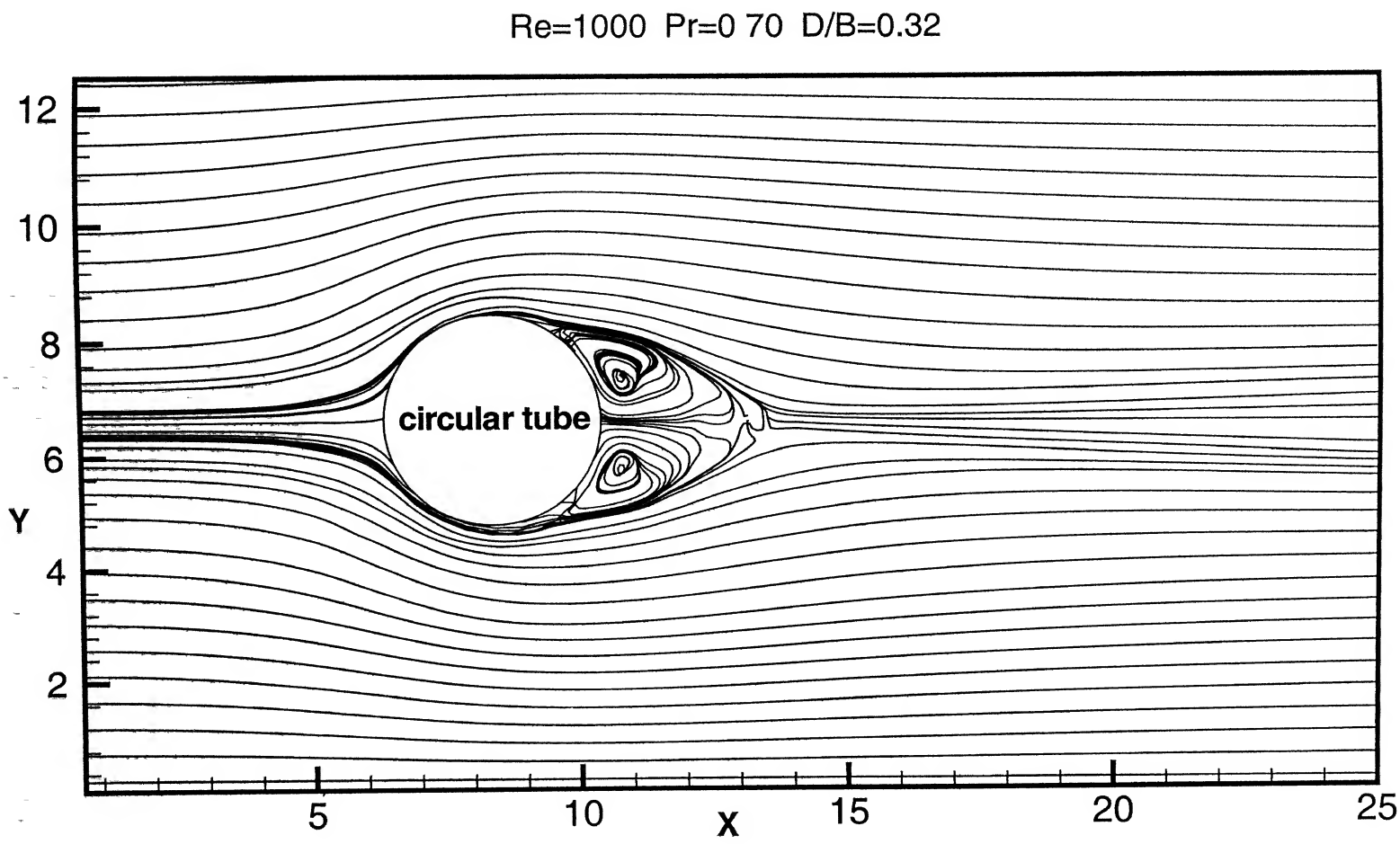

Figure 5.12 Steamline plot at the mid-plane between channel wall and annular fin

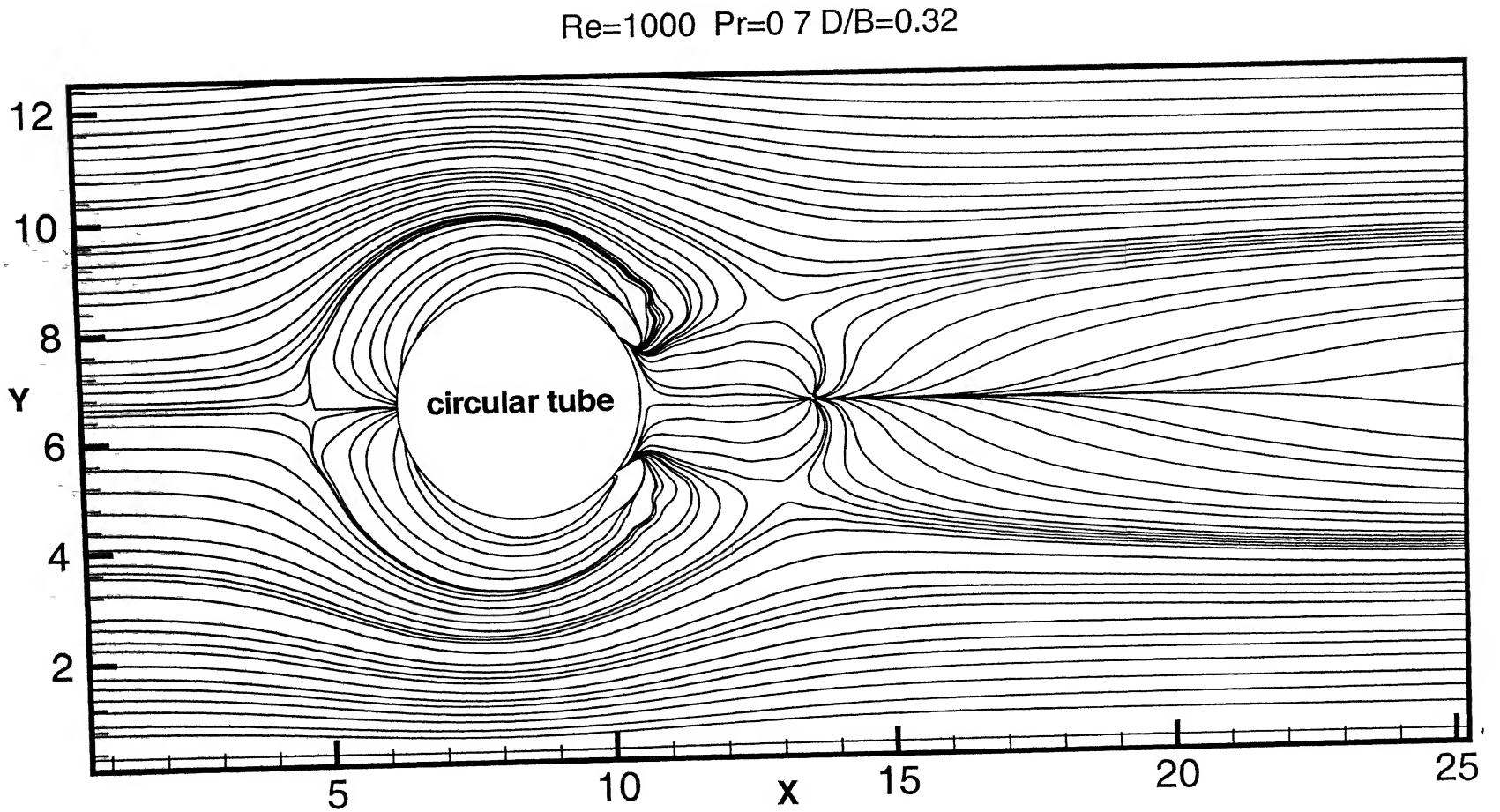

Figure 5.13 Streamline very near to the bottom wall of the channel

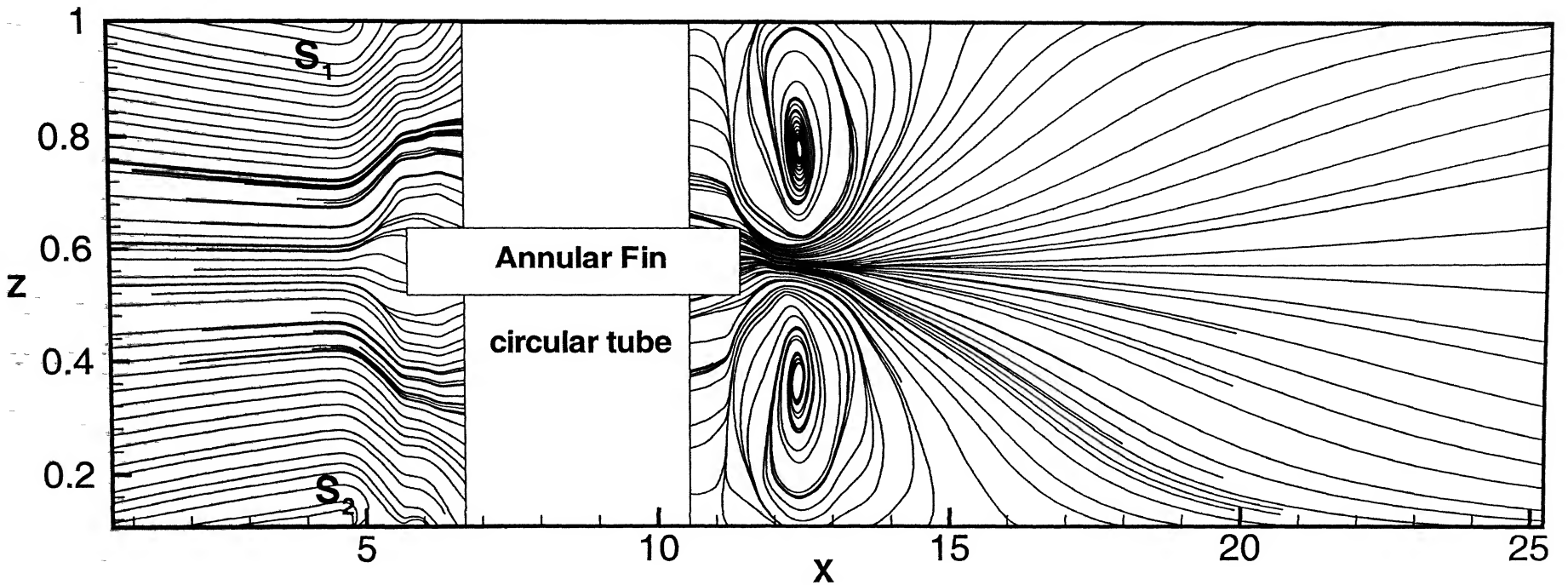

Figure 5.14 Streamline at the vertical mid-plane (Z-X)

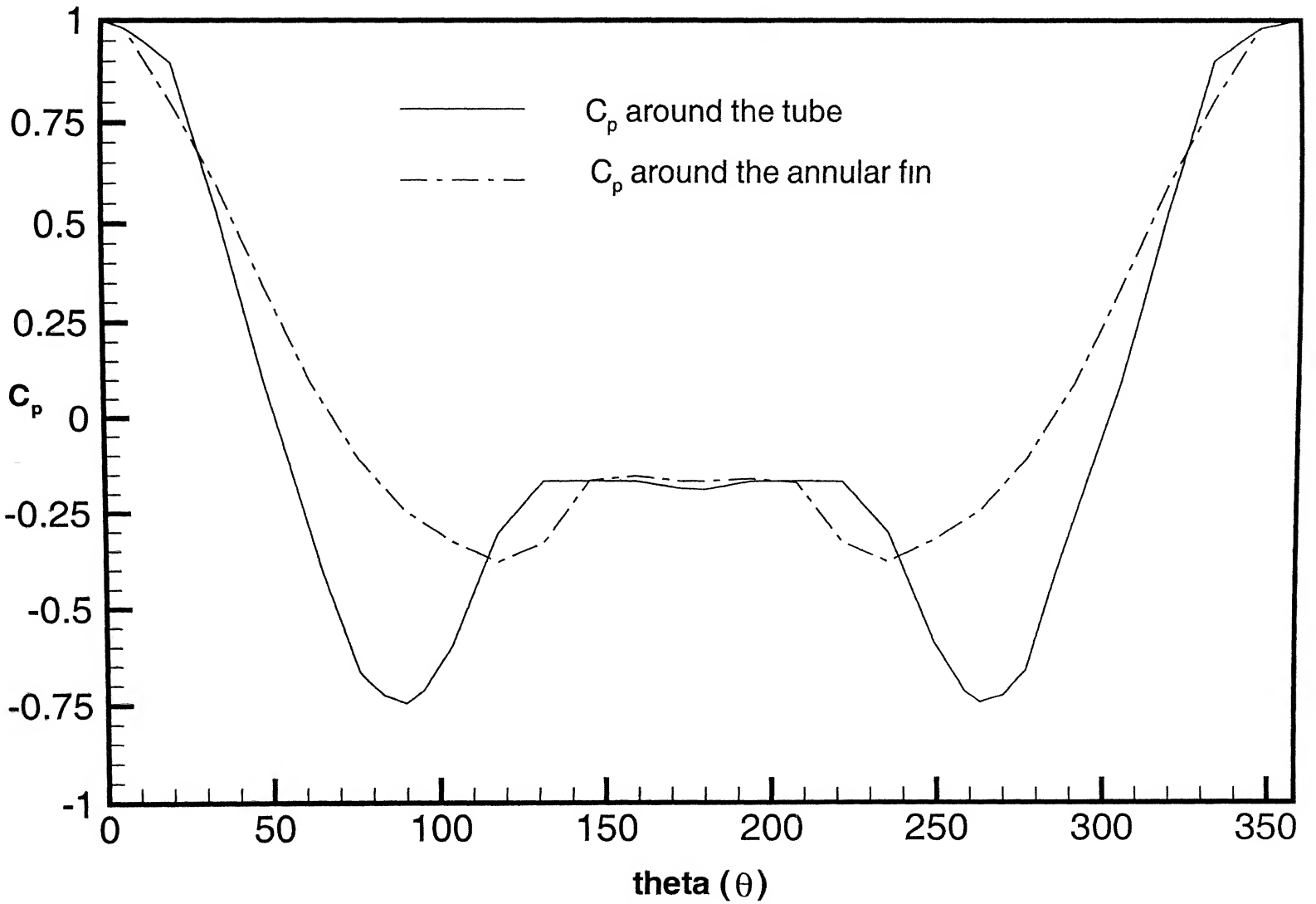

Figure 5.16 Distribution of pressure coefficient around the tube with annular fin at different positions

5.3.2 Heat Transfer Characteristics

In this section the heat transfer characteristics for the annular fin is discussed

Temperature Distribution

Figure 5 17 shows the temperature distribution on the vertical midplane of the channel This figure reveals the development of thermal boundary layer along the top and bottom plate The contour plot is symmetric with respect to $z = H/2$ The effect of the annular fin on the temperature contours is observed in this figure

Figure 5 18 represents the temperature contours at the cross strem plane at a location $x = l_c$ This figure shows how the plates and the annular fin influences the temperature of the fluid

Nusselt Number Distribution

Figure 5 19 Represents the contour map of local Nusselt number very close to the bottom plate and the top plate These two plots are identical. There are some issues which are to be addressed before hand In practice, the tube, channel walls and the fin do not have constant temperature because both convective and conductive heat transfer take place from the tube, channel walls and the fin In the present computation, it is assumed that all (tube, channel walls and the annular fin) are at the constant temperatue At the leading edge of the bottom plate, Nusselt number has its maximum value and it decreases gradually upto some location infront of the tube At the inlet, the cooler fluid comes in contact with the hot solid wall for the first time and the temperature difference is maximum. The Nusselt number reveals highest value herein The thermal boundary layer

developes downstream The formation of thermal boundary layer causes decrease in heat transfer rate and the Nusselt number decreases There is a sudden increase in Nusselt number in front of the tube The reason for the sudden increase in Nusselt number can be attributed to the formation of horseshoe vortices The spiraling motion of the horseshoe vortices brings about a better mixing and the heat transfer in this region is enhanced significantly

The local Nusselt number distribution on the top and bottom side of the annular fin is shown in Figure 5 20 The Nusselt number distribution pattern at the top surface of the annular fin is same as that for the bottom surface Here, at the extreme left, the relatively colder fluid comes in contact with the heated fin surface The heat transfer is maximum here As the fluid moves above and below around the fin surface, its temperature increases and Nusselt number on the surfaces decreases

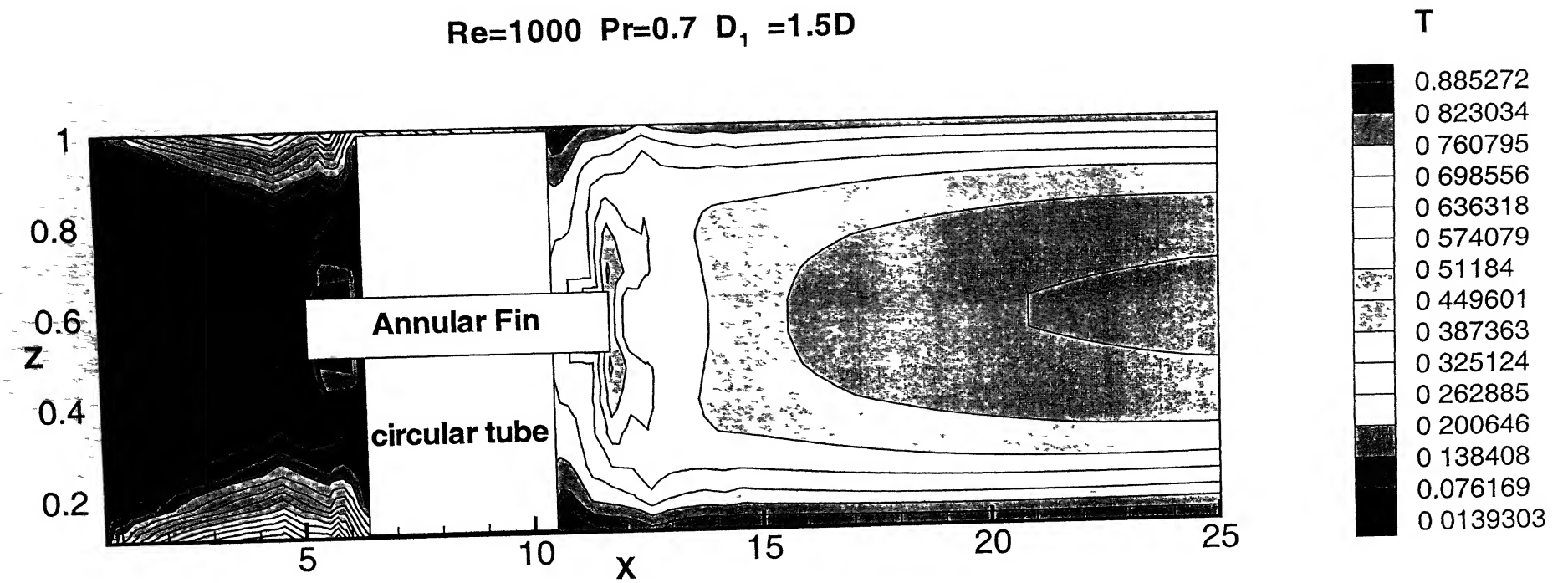

Figure 5.17 Temperature distribution at the plane(Z-X) cut through the centre of the tube

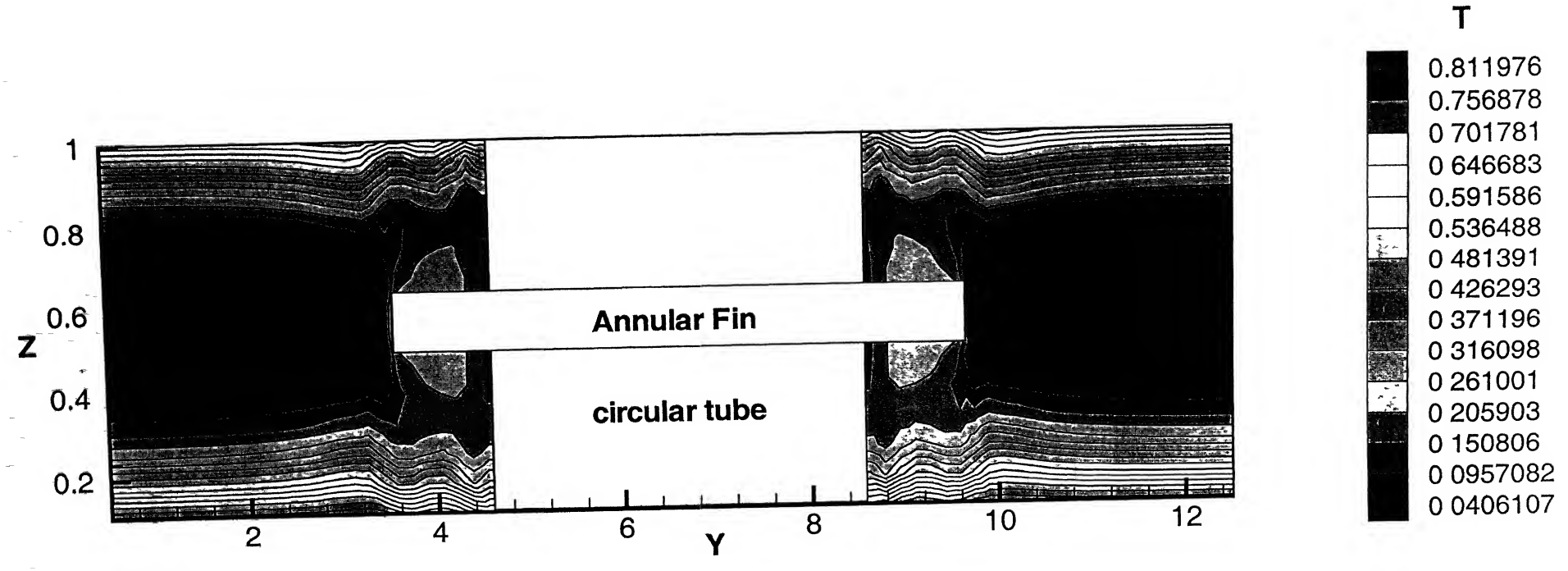

Figure 5.18 Temperature distribution at the vertical plane (Y-Z) cut through the centre of the tube.

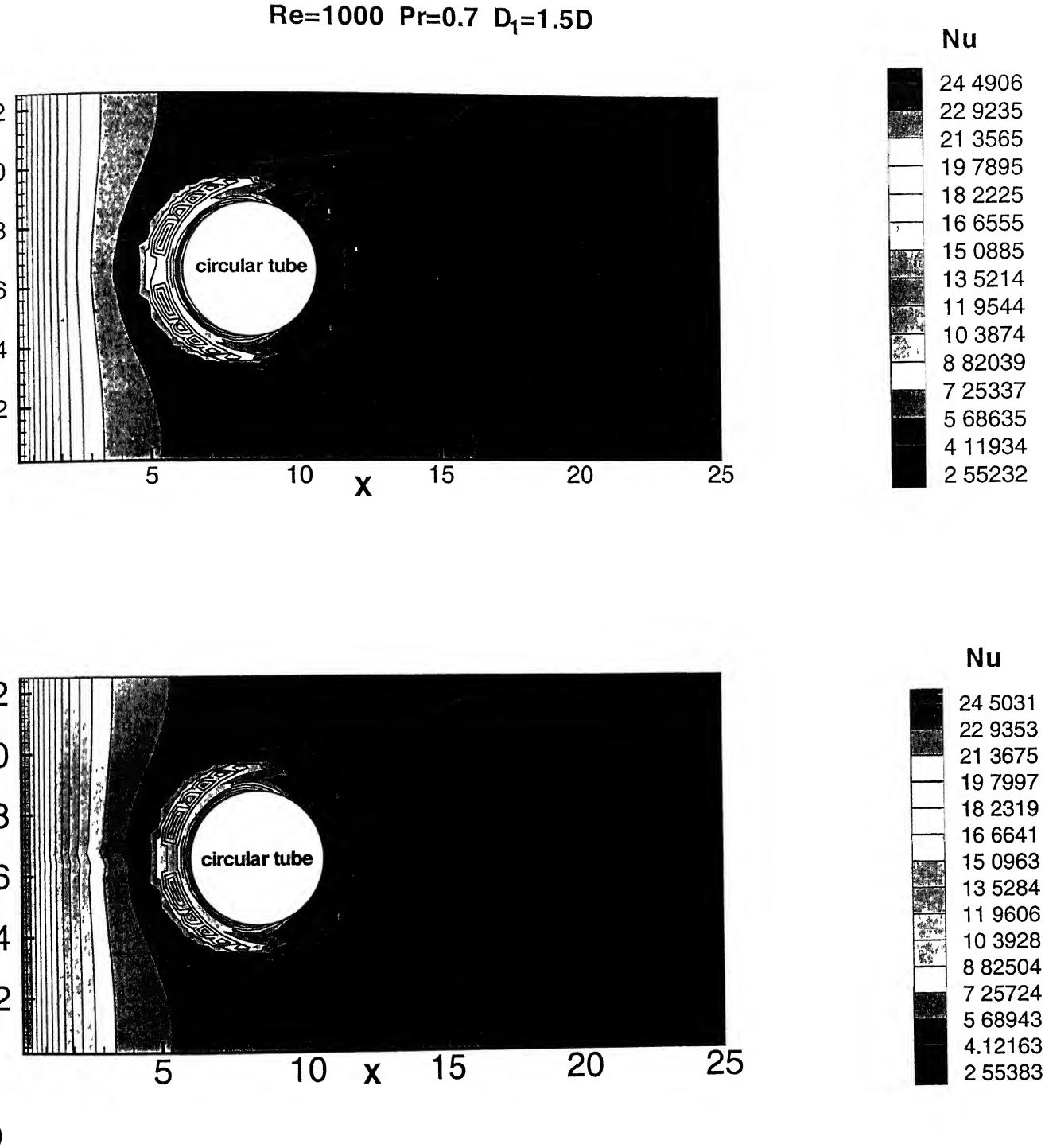

Figure 5.19 Iso-Nusselt number distribution at the (a) bottom plate &(b) top plate

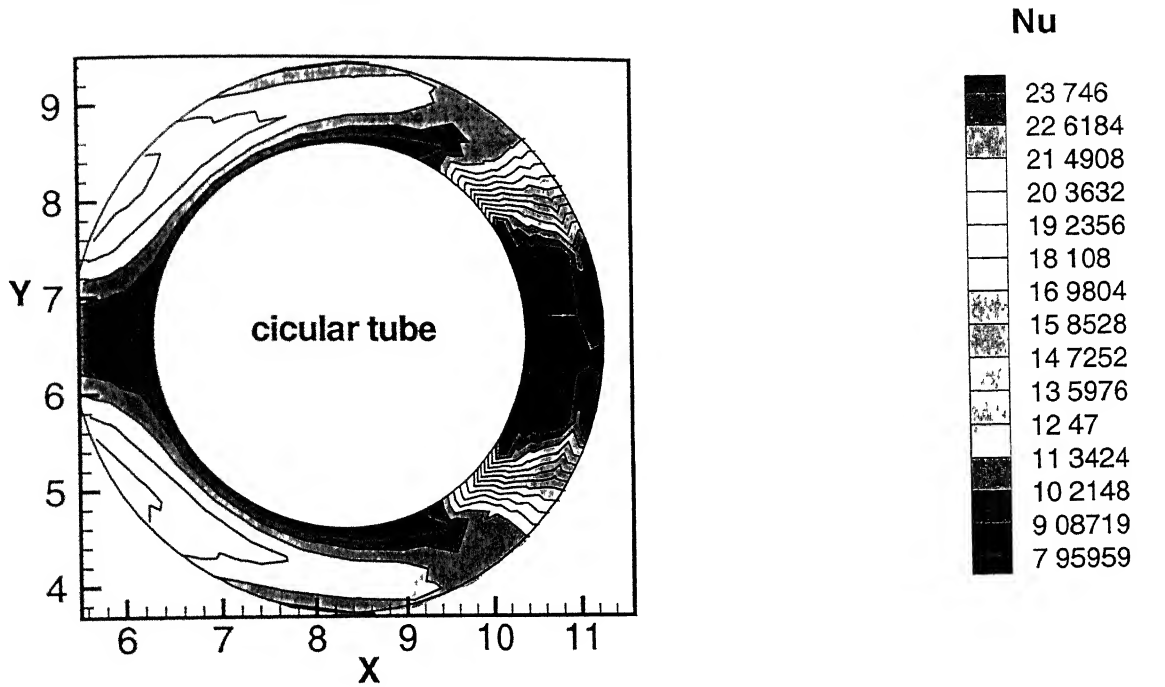

(a)

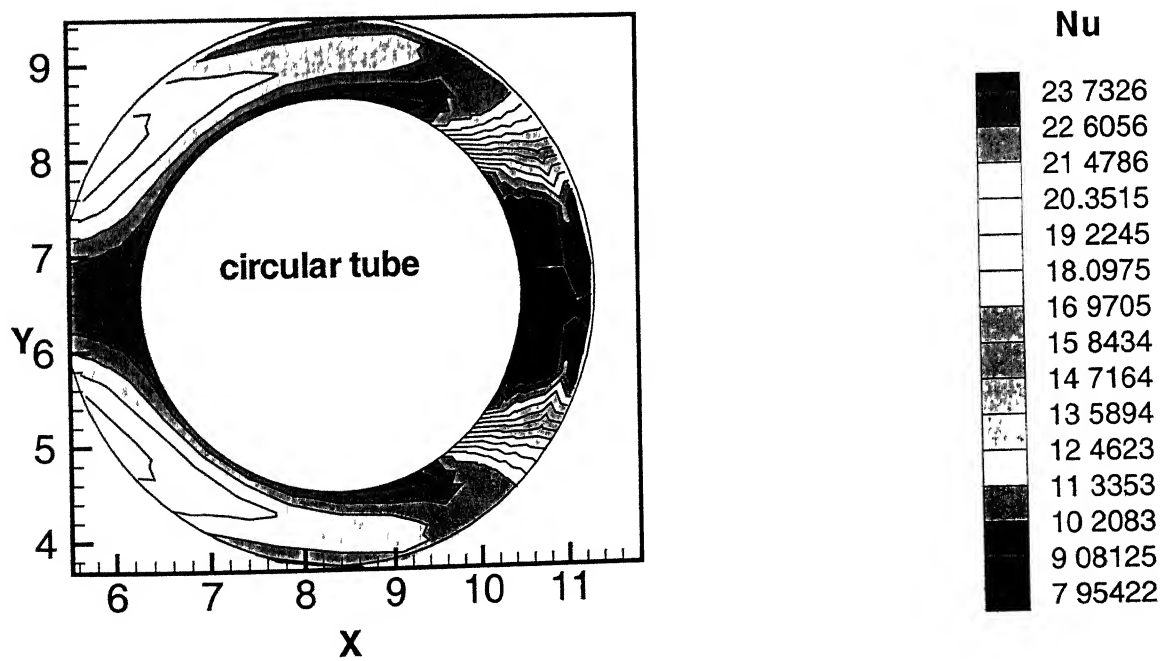

(b)

Figure 5.20 Nusselt number variation of the Annular Fin
(a) at the top surface
(b) at the bottom surface

5.4 Model Validation

The model validation was performed through comparison with the experimental results of Eckert and Soehngen (1952) and numerical results of Chun and Boehm (1989) for a Reynolds number of 218 Figure 5 21 shows the comparison of local Nusselt numbers along the circumference of the tube Present computation compares favourably with the experiments of Eckert and Soehngen (1952)

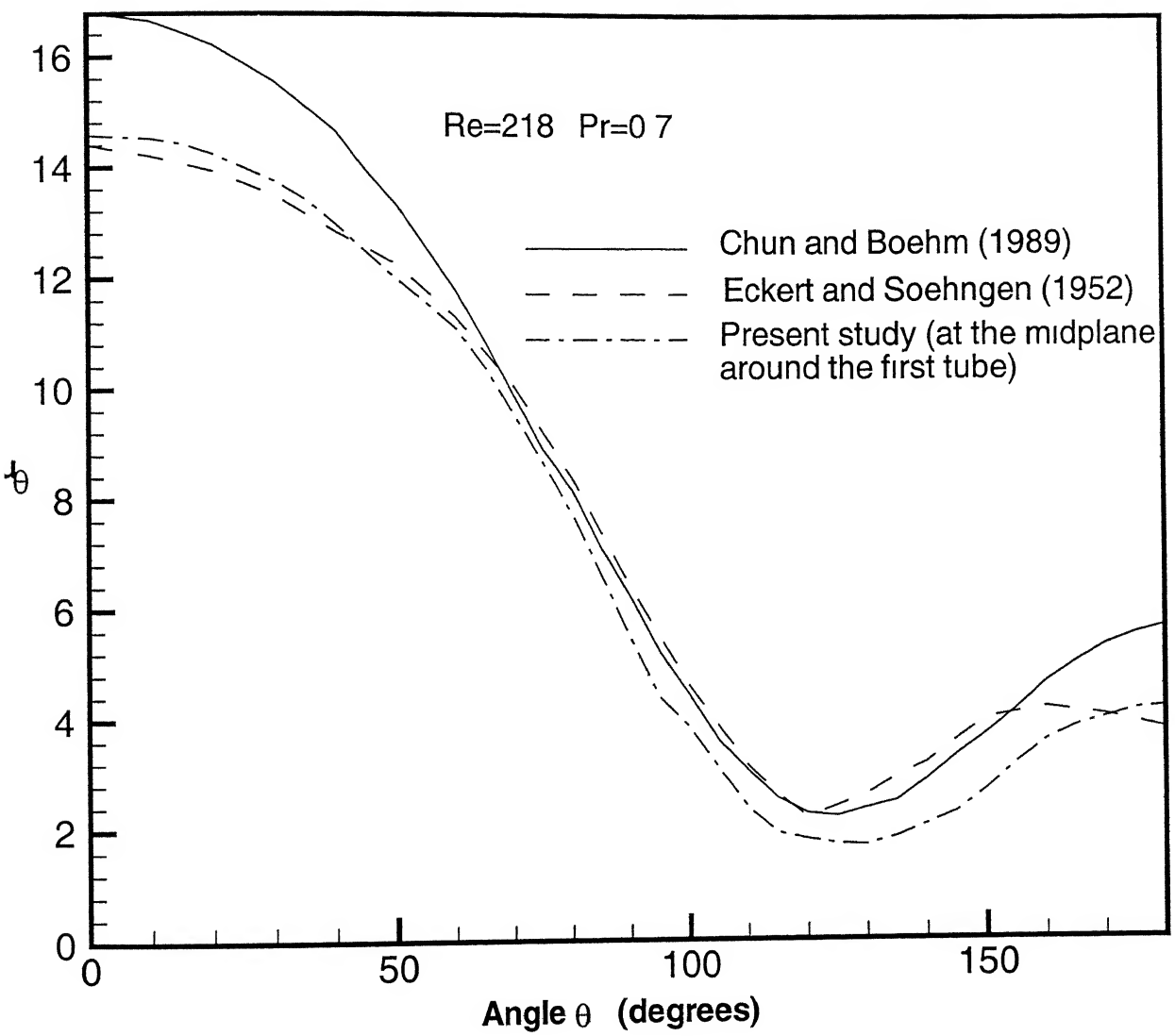

Figure 5.21 Comparison of local Nusselt number distribution on the tube surface

Chapter 6

Conclusions and Scope for Future Work

6.1 Conclusion

A three-dimensional computational study of forced convection heat transfer has been carried out to determine the flow and heat transfer characteristics The full Navier-Stokes equations together with the energy equation are expressed in integral form A semi-explicit control volume formulation of Eswaran and Prakash (1998) is used to solve the governing equations This study focuses on the detailed analysis of the flow and heat transfer characteristics in a rectangular channel with a built-in circular tube having a longitudinal fin, i e , Splitter Plate and a built-in circular tube having a circumferential fin,i e , Annular Fin

Particular attention has been paid to the variation of coefficient of pressure, coefficient of drag, vortex structure, limiting streamlines and heat transfer with splitter plate length This study has shown that the characteristics of the wake downstream of a circular tube can be considerably altered by placing a splitter plate on the wake centerline downstream of the circular tube Flow visualization indicated that a splitter plate reduced the level of 3-dimensionality in the formation region by stabilizing the transverse 'flapping' of the shear layers The use of splitter plate streamlines the flow Thus the vortices are pushed downstream, which decreases the heat transfer But again the presence of splitter plate in-

creases the heat transfer area substatially by complementing for conduction heat transfer This results in an overall enhancement in heat transfer The splitter plate being a slender body in the shown configuration, tends to decrease even the pressure loss penalty A circular tube with an annular fin causes a significant change in the temperature field of the channel The presence of annular fin increases the heat transfer area The Nusselt number distribution on the top and the bottom surfaces of the annular fin shows the pattern which is quite similar to that of bottom and top wall of the channel The pressure distribution around the annular fin is quite similar to that of a circular tube

6.2 Scope for Future Work

The results are presented for the case of splitter plate of lengths ($L = 2H, 3H$ and $4H$). This work may be extended to solve the problem when length of the splitter plate will be more or less than the present case It may be possible to use sinuous trailing edge splitter plate Also the circular tube could be replaced by oval tube We can try to extend this to show the effects of splitter plate for very high Reynolds number We can aim for finding out the length of the splitter plate for which there would be maximum heat transfer corresponding to a given Reynolds number The effect of the length of a splitter plate on Strouhal number may be a interesting study to be investigated Here in the present computational study only a circular tube placed in a channel has been considered. This study can be extended for the tube banks

A circular tube with an annular fin of outer diameter of 1 5D has been investigated. This work can be extended for the different outer diameter of the annular fin This study would be attractive if it is extended by attaching two or more fin in the prescribed geometry

Bibliography

[1] Achaichia, A and Cowell, T W (1988), Heat Transfer and Pressure Drop Characteristics of Flat Tube and Louvered Plate Fin Surfaces,*Experimental* Thermal and Fluid Science, Vol. 1, pp 147-157

[2] Acharya, S , Myrum, T A and Inamdar, S (1991), Sub-harmonic Excitation of the Shear layer between Two Ribs Vortex Interaction and Pressure Field, *AIAA* J , Vol 29, pp 1390-1399

[3] Amon, C H and Patera, A T (1989), Numerical Calculation of Stable Three-Dimentional Tertiary States in Grooved-Channel Flow, *The* Physics of Fluids-A , Vol 35, pp 803-814.

[4] Anderson, E A and Szewczyk, A. A , Effects of a splitter plate on the near wake of a circular cylinder in 2 and 3 dimensional flow configurations, *Experiments* in Fluids, Vol 23, pp 161-174, 1997

[5] Apelt, C J , Isaacs, L. T., Effects of Splitter Plates Placed in the Wake of Bluff Cylinders, *C*A.A R.C. Symposium on Separated Flows and Wakes, University of Melbourne, Melbourne, Australia, 1970

[6] Apelt, C J , West, G S.,and Szewczyk, A A., The effects of wake splitter plates on the flow past a circular cylinder in the range of $10000 < Re < 50000$., *J* Fluid Mech , Vol 61, pp 187-198, 1973

[7] Apelt, C J , West, G S , The Effects of Wake Splitter Plates on Bluff-Body Flows in the Range $10^4 < Re < 5 \times 10^4$,Part 2, *J* Fluid Mech , Vol 71, pp 145-160, 1975

[8] Basu, S , Eswaran, V and Biswas, G (2001), Numerical prediction of Flow and Heat Transfer in a Rectangular with a Built-in Circular Tube, *P*roceedings of IMECE, New York City, USA

[9] Baker, C T , The laminar horseshoe vortex, part 2, *J* Fluid Mech , Vol 95, pp 347-367, 1979

[10] Bearman, P W , Investigation of the Flow Behind a Two-Dimensional Model with a Blunt Trailing Edge and Fitted with Splitter Plates, *J*ournal of Fluid Mechanics, Vol 21, 1965, pp 241-255

[11] Biswas, G and Chattopadyay, H (1992), Heat Transfer in a Channel with Built in Wing-type Vortex Generators, *I*nt J Heat And Mass Transfer, Vol 35, pp 803-814

[12] Biswas, G and Mitra, N K (1998), Longitudinal Vortex Generators for Enhancement of Heat Transfer in Heat Exchanger Applications, *P*roc 11^th Int J Heat Transfer Conference, Kyongju, Vol 5, pp 339-344

[13] Biswas, G and Mitra, N K and Fiebig, M (1994),Heat Transfer Enhancement in Fin-Tube Heat Exchangers by Winglet-type Vortex Generators, *I*nt J Heat And Mass Transfer, Vol 35, pp 283-294

[14] Biswas, G , Torii, K , Fujii, D and Nishino, K (1996), Numerical and experimental determination of flow structure and heat transfer of longitudinal vortices in a channel flow, *I*nt J Heat And Mass Transfer, Vol 39, No. 16, pp 3441-3451

[15] Eibeck, P A and Eaton, J , K , Heat Transfer Effects of a Longitudinal Vortex Embedded in a Turbulent Shear Flow, *J*ournal of Heat Transfer, Vol 109, pp 16-24, 1986

[16] Eswaran, V and Prakash, S , A Finite Volume Method for Navier-Stokes Equations, Proceedings of the Third Asian CFD Conference, Bangalore, Vol 1, pp 127-133, 1998

[17] Fiebig, M , Kallweit, P and Mitra, N K , Wingltype Vortex Generators for Heat Transfer Enhancement, *P*roceedings of the Eighth International Heat Transfer Conference, San Fransico, Vol 6, pp 2909-2913, 1986

[18] Fiebig, M , Brockmeier, U , Mitra, N K and Guntermann, T , Structure of velocity and temperature fields in laminar channel flows with longitudinal vortex generators, *N*umerical Heat Transfer, Part A, Vol 15, pp 281-302, 1989

[19] Fiebig, M , Kallweit, P , Mitra, N K and Tiggelbeck, S , Heat Transfer Enhancement and Drag by Longitudinal Vortex Generators in Channel Flow, *E*xperimental Thermal and Fluid Science, Vol 4, pp 103-114, 1991

[20] Fisher, E. M and Eibeck, P A , The influence of a horseshoe vortex on local convective heat transfer, *A*SME J Heat Transfer, Vol. 112, pp 329-335, 1990

[21] Gerrard, J H , The mechanics of the formation region of vortices behind bluff bodies,*J* Fluid Mech , Vol 25, pp 401, 1965

[22] Goldstein, R J., and Karni,J , The effect of a wall boundary layer on a local mass transfer from a cylinder in cross flow,*J*ournal; of Heat Transfer(ASME),Vol 106, pp 260-267, 1984

[23] Harlow, F H and Welch, W. E., Numerical Calculation of Time-Dependent Viscous Incompressible Flow of Fluid with Free Surface, *T*he Phys Fluids, Vol 8, pp 2182-2188, 1965.

[24] Hirt,C W , and Cook,J L , Calculating Three-Dimensional Flows around Structures and over Rough Terrain, *J* Comp Phys ,Vol 10, pp 324-340, 1972

[25] Kaul,U K , Kwak,D , and Wagner,C , A Computational Study of Saddle Point Separation and Horseshoe Vortex System, *A*IAA'85-0812Reno,Nevada,1985

[26] Kawai, H , A discrete vortex analysis of flow around a vibrating cylinder with splitter plate J Wind Engr and Ind Aero ,Vol 35, pp 237-273

[27] Kim,S , and Benson,T J , Comparison of SMAC,PISO and Iterative Time-Advancing Schemes for Unsteady Flows, *C*omputers and Fluids ,Vol 21,pp 435-454,1992

[28] Kobayashi,M H , and Pereira,C F , Calculation of Incompressible Laminar Flows on a Non-staggered,Non-Orthogonal Grid, *N*umerical Heat Transfer,part B,Vol 19, pp 243-262, 1991

[29] Majumder,S , Role of under-relaxation in momentum interpolation for calculation of flow with non-staggered grids, *N*umerical Heat Transfer ,Vol 13, pp 125-132, 1998

[30] Mansingh, V and Oosthuizen, P H , Effects of splitter plates on the wake flow behind a bluff body, *A*IAA Journal, Vol 28, pp 778-783, 1990

[31] Mansingh, V , Experimental Investigation of Effects of Splitter Plates on the Flow Behind a Rectangular Cylinder, Ph D Thesis, Queen's University, Kingston, Canada, 1986

[32] Mukhopadhyay,A , Sunderrajan,T , and Biswas,G., An Explicit Transient Algorithm for Predicting Incompressible Viscous Flows in Arbitrary Geometry, *I*nt J Heat and Mass Transfer,Vol 41, pp. 3829-3840,1993

[33] Orlanski, I , A Simple Boundary Condition for Unbounded Flows, *J* Comput Phys , Vol 21, pp 251-269, 1976

[34] Patankar,S V and Spalding, D B , A Calculation Procedure for Heat, Mass and Momentum Transfer in Three-Dimensional parabolic Flows, *I*nt J Heat Mass TransferVol 15, pp 1787-1806,1972

[35] Peric, M , A Finite Volume Method for the Prediction of Three-Dimensional Fluid Flow in Complex Ducts,*P*h D ,Thesis,University of London

[36] Peric,M , Kessler,R , and Scheuerer,G , Comparison of finite-volume numerical methods with Staggered and Collocated Grids, *C*omputers and Fluids,Vol 16,pp 389-403,1988

[37] Prabhakar, V , Biswas, G and Eswaran, V , Numerical Prediction of Heat Transfer in a Channel with a Built-in Oval Tube and Two Different Shaped Vortex Generators, *N*umerical Heat Transfer, Part A, Vol 41, pp 307-329, 2002

[38] Roshko, A , On the drag and shedding frequency of two-dimensional bluff bodies, *N*ACA TN3169, 1954

[39] Roshko, A , On the Wake and Drag of Bluff-Bodies,*J*ournal og Aeronautical Science, Vol 22, 1955,pp 124-137

[40] Saboya, F E M and Sparrow, E M , Local and average transfer coefficients for one-row plate fin and tube heat exchanger configurations, *J*. Heat Transfer, Vol 96, pp 265-272, 1974

[41] Sanchez, M , Mitra, N., K and Fiebig, M , Numerical investigation of three-dimentional laminar flows in a channel with built-in circular cylinder wing-type vortex generators, *P*roc. Eighth GAMM-Conference on numerical methods, Vieweg Verlag, pp 484-492, 1989.

[42] Shah, R ,K and London, A ,L , Laminar Flow Forced Convection in Ducts,*A*dvances in Heat Transfer, Suppl 1, pp 169-176, Academic Press, New York (1978)

[43] Sohankar, A , Davidson,L , and Norberg,C , Simulation of Unsteady Three-Dimensional Flow around a Square Cylinder at Moderate Reynolds Number, *P*hys of Fluids ,Vol 11,No 2,pp 288-306,1999

[44] Sohankar, A , Davidson,L , and Norberg,C , arge Eddy Simulation of Flow Past a Square Cylinder Comparison of different Subgrid Scale Models, *T*rans ASME J Fluids Engrg ,Vol 122,No 1,pp 39-47,2000

[45] Sparrow, E M and Kang, S S , Longitudinally-finned cross-flow tube banks and their heat transfer and pressure drop characteristics, *I*nt J of Heat Mass Transfer, Vol 28, No 2, pp 339-350, 1985

[46] Sparrow, E , M and Chastian, S , R , Effect of angle of attack on the heat transfer coefficient for an annular fin,*I*nt J Heat Mass Transfer, Vol 29, pp 1185-1191, 1986

[47] Sung, H ,J , Yang, J , S and Park, T , S , Local convective mass transfer on circular cylinder with transverse annular fins in crossflow,*I*nt J Heat Mass Transfer, Vol 39, No 5, pp 1093-1101, 1996

[48] Tigglebeck, S , Mitra, N , K and Fiebig, Flow structure and heat transfer in a channel with multiple longitudinal vortex generators,*E*xp Thermal Fluid Science, Vol 5, pp 425-436, 1992

[49] Van Doorthal,J P , and Raithby,G D , Enhancement of the SIMPLE method for Predicting Incompressible Fluid Flows, *N*umerical Heat Transfer ,Vol. 7,pp 147-163, 1984

[50] Vanka,S P , Second-Order Upwind Differencing in a Recirculating Flow,*A*IAA J ,Vol 17,pp 1079-1096,1987.

[51] Velusamy,K , and Garg,V K , Entrance Flow ın Ellıptıc Ducts, *I*nt J Numerıcal Methods ın Fluıds, Vol 17, pp 1079-1096,1993

[52] Vıcellı,A J , A Computıng Method for Incompressıble Flows Bounded by Movıng Walls,*J* Comp Phys , Vol 8,pp 119-143, 1971

[53] Yanagıhara, J , L and Torıı, K , Heat Transfer Characterıstıcs of Lamınar Boundary Layer ın the Presence of Vortex Generators, *P*roceedıngs of the Nınth Internatıonal Heat Transfer Conference, Vol 6, pp 323-328, 1990